THE EFFECT OF NI ON THE MICROSTRUCTURE, WEAR AND CORROSION BEHAVIORS OF MICROALLOYED STEELS PRODUCED BY POWDER METALLURGY

2023
DOCTORAL THESIS
MECHANICAL ENGINEERING

Mohamed Ahmed AHSSI

Thesis Advisor
Assoc. Prof. Dr. Mehmet Akif ERDEN

THE EFFECT OF NI ON THE MICROSTRUCTURE, WEAR AND CORROSION BEHAVIORS OF MICROALLOYED STEELS PRODUCED BY POWDER METALLURGY

Mohamed Ahmed AHSSI

Thesis Advisor

Assoc. Prof. Dr. Mehmet Akif ERDEN

T.C.

Karabuk University

Institute of Graduate Programs

Department of Mechanical Engineering

Prepared as

Doctoral Thesis

KARABUK

February 2023

APPROVAL

I certify that, in my opinion, the thesis submitted by Mohamed Ahmed AHSSI titled "THE EFFECT OF NI ON THE MICROSTRUCTURE, WEAR AND CORROSION BEHAVIORS OF MICROALLOYED STEELS PRODUCED BY POWDER METALLURGY" is fully adequate in scope and quality as a thesis for the degree of Doctor of Science.

Assoc. Prof. Dr. Mehmet Akif ERDEN .....

Thesis Advisor, Department of Mechanical Engineering

This thesis is accepted by the examining committee with a unanimous vote in the Department of Mechanical Engineering as a Doctoral of Science thesis. 16.01.2023

Examining Committee Members (Institutions)	Signature
Chairman: Prof. Dr. Mustafa ACARER (SU)	.....
Member: Assoc.Prof.Dr. Mehmet Akif ERDEN (KBU)	.....
Member: Assoc.Prof.Dr. Harun ÇUĞ (KBU)	.....
Member: Assist. Prof. Dr. Muhammed ELİTAŞ (BŞU)	.....
Member: Assist. Prof. Dr. Adem Fatih ÖZALP (KBU)	.....

The degree of Doctoral of Science by the thesis submitted is approved by the Administrative Board of the Institute of Graduate Programs, Karabuk University.

Prof. Dr. Müslüm KUZU .....

Director of the Institute of Graduate Programs

"*I declare that all the information within this thesis has been gathered and presented in accordance with academic regulations and ethical principles, and I have cited all those according to the requirements of the regulations and principles, which do not originate in this work*."

Mohamed Ahmed AHSSI

ABSTRACT

Ph.D. Thesis

THE EFFECT OF NI ON THE MICROSTRUCTURE, WEAR AND CORROSION BEHAVIORS OF MICROALLOYED STEELS PRODUCED BY POWDER METALLURGY

Mohamed Ahmed AHSSI

Karabük University
Institute of Graduate Programs
The Department of Mechanical Engineering

Thesis Advisor:
Assoc. Prof. Dr. Mehmet Akif ERDEN
February 2023, 77 pages

Microalloyed steels can be stated as low-alloyed high-strength steels that improve the mechanical properties of the carbide, nitride and carbonitride formed by the addition of carbide and nitride-forming elements such as titanium, niobium and vanadium, which are added below 0.2% by weight. The formation and dissolution temperatures of carbon nitrides formed in microalloy steels must be calculated very well. Otherwise, incorrectly designed casting method, rolling temperature and cooling rate may cause carbonitrides not to form or to form and overgrow. The production of microalloyed steels produced by rolling, controlled cooling and casting methods has also been carried out by powder metallurgy method in recent years. Powder metallurgy is one of the independent production methods that is used in the manufacture of parts used in many sectors such as implant materials, gears, tortoiseshells, bushings, which cannot be produced with other production methods such as tungsten filament used in electric

lamps, including small precision parts that are difficult to manufacture. The element nickel added in this study is an austenite stabilizer and widens the austenite area as well as narrowing the ferrite area in iron chromium carbon alloys. Nickel increases corrosion resistance against oxidation at high temperatures. It prevents scale formation on the material surface. In addition, nickel, which has a grain reduction effect, increases the toughness and strength of the material. It increases the hardness, ductility, high fatigue resistance of the material and decreases the critical cooling rate by using it with chromium. Compared to many elements such as carbon, copper and molybdenum, the nickel element diffuses slowly in iron because its diffusion coefficient value is lower. In this study, alloy steel with nine different compositions was produced by adding graphite, Nb, V and Ni in different proportions into Fe powders. Characterization of alloy steel samples containing different amounts of Nickel was carried out by corrosion test, wear test, hardness test, optical microscope, XRD, SEM Mapping and SEM EDS analyses.

Keywords : Powder metallurgy, Microalloyed steels, Nickel, Corrosion, Wear, Microstructure.

Science Code : 91437

ÖZET

Yüksek Lisans Tezi

TOZ METALÜRJİSİ İLE ÜRETİLEN NB-V MİKROALAŞIMLI ÇELİKLERE Nİ İLAVESİNİN AŞINMA VE KOROZYON ÖZELLİKLERİNE ETKİSİ

Mohamed Ahmed AHSSİ

Karabük Üniversitesi
Fen Bilimleri Enstitüsü
Makine Mühendisliği Anabilim Dalı

Tez Danışmanı:
Doç. Dr. Mehmet Akif ERDEN
February 2023, 77 sayfa

Mikroalaşımlı çelikler ağırlık olarak %0,2'nin altında katılan titanyum, niyobyum ve vanadyum gibi karbür ve nitrür yapıcı elementlerin ilavesi ile oluşturmuş olduğu karbür, nitrür ve karbonitrürlerin çeliğin mekanik özelliklerini iyileştiren düşük alaşımlı yüksek dayanımlı çelikler olarak ifade edilebilir. Mikroalaşım çeliklerinde oluşan karbo-nitrürlerin oluşma ve çözünme sıcaklıklarının çok iyi hesaplanması gerekmektedir. Aksi taktirde yanlış tasarlanan döküm yöntemi, haddeleme sıcaklığı ve soğuma hızı karbonitrürlerin oluşmamasına veya oluşup aşırı büyümesine sebep olabilir. Haddeleme, kontrollü soğutma ve döküm yöntemleriyle üretilen mikroalaşımlı çeliklerin üretimi son yıllarda toz metalurjisi yöntemiyle de gerçekleştirilmektedir. Toz metalürjisi imali zor küçük hassas parçalar da dahil olmak üzere elektrik lambalarında kullanılan tungsten filament gibi diğer üretim yöntemleri ile üretilemeyen, implant malzemeleri; dişli, bağa, burç gibi birçok sektörde kullanılan

parçaların imalinde kullanılan, her geçen gün kullanım alanı gelişmekte olan müstakil üretim yöntemlerinden biridir. Bu çalışmada ilave edilen nikel elementi ise östenit dengeleyicidir ve demir krom karbon alaşımlarında ferrit alanını daraltmasının yanı sıra östenit alanını genişletmektedir. Nikel yüksek sıcaklıklarda oksitlenmeye karşı korozyon direncini artırır. Malzeme yüzeyinde tufal oluşumunu engeller. Ayrıca tane küçültme etkisine sahip olan nikel, malzemenin tokluğunu ve mukavemetini artırır. Krom ile kullanılması ile malzemenin sertliğini, sünekliliğini yüksek yorulma direncini artırır ve kritik soğuma hızını düşürür. Nikel elementi karbon, bakır ve molibden gibi birçok element ile karşılaştırıldığında, sahip olduğu difüzyon katsayısı değeri daha düşük olduğundan demir içerisinde yavaş yayınım gösterir. Bu çalışmada Fe tozlarının içerisine grafit, Nb, V ve farklı oranlarda Ni ilave edilerek dokuz farklı bileşime sahip alaşımlı çelik üretimi gerçekleştirilmiştir. Farklı oranlarda Nikel içeren alaşımlı çelik numunelerin karakterizasyonu korozyon testi, aşınma testi, sertlik testi, optik mikroskop, XRD, SEM Maping ve SEM EDS analizleri ile gerçekleştirilmiştir.

Anahtar Sözcükler: Toz metalurjisi, mikroalaşımlı çelikler, Nikel, Korozyon, Aşınma, mikroyapı.

Bilim Kodu **:** 91437

ACKNOWLEDGMENT

First of all, I want to thank my mentor and adviser, Assoc. Prof. Dr. Mehmet Akif ERDEN, for all of his help, interest, and advice in helping me conduct and report this research. I can't explain how grateful I am for his insightful advice and encouragement.

I also like to thank all the lecturers at Karabuk University who helped me by offering further advice. For their enormous contributions to my education, the university staff, the Turkish government, and the Turkish people deserve my sincere gratitude.

I also thank my wife in particular for her time, emotional support, and inspiration throughout my studies. I also want to thank my entire family for their help, prayers, and tolerance while I was studying.

CONTENTS

Page

Page

Page

LIST OF FIGURES

Page

Page

LIST OF TABLES

Page

SYMBOLS AND ABBREVITIONS INDEX

SYMBOLS

Ni : Nickel
Mo : Molybdenum
V : Vanadium
Mn : Manganese
Cr : Chromium
Fe : Iron
Ti : Titanium
Nb : Niobium
C : Carbon
Mg : Magnesium
O : Oxygen
N : Nitrogen

ABBREVIATIONS

PM : Powder Metallurgy
EDS : Energy Dispersive X-Ray Spectroscopy
SEM : Scanning Electron Microscopy
XRD : X-ray powder diffraction
ISO : Standardization of International Organization

PART 1

INTRODUCTION

Micro-alloyed steels are a steel category that contains vanadium, niobium, aluminum, and titanium in micro quantities (0.05-0.20wt %). The qualities of the micro-alloyed steels are noticeably better, with greater toughness and strength, good weldability, higher corrosion resistance, and lower ductile-to-brittle transition temperature. Applying appropriate thermo-mechanical techniques and a number of hardening mechanisms, the mentioned attributes were obtained. Powder metallurgy is needed for the manufacturing of items such as aircraft parts, automobile spare parts, electrical connection components, nuclear power plants, high-temperature filters, armor-piercing materials, clock parts, orthopedic materials, high-power lighting, and jet engines [1].

For its manufacturability, economy, quality, high performance, uniformity, and cheap production costs, powder metallurgy, or PM, is a useful production technique. Because nickel is an austenite stabilizer, it causes the austenite area of steel to grow while the ferrite region of steel contracts. Additionally, it increases the oxidation and corrosion resistance at high temperatures. By refining the grain size, nickel improves strength and toughness and prevents scale formation on the surface. If it is used with chromium, it increases ductility, hardness, critical cooling rate, and fatigue resistance. As a significant element on the Periodic Table, Nickel has a lower diffusion coefficient, and if we compare it to other elements, it diffuses into iron at a slower rate [2].

The existing literature shows adequate research on PM steel production, its mechanical properties, corrosion behavior, microstructure, and the interrelationship between the mentioned factors. The PM method has been declared useful in many of them. For instance, Erden applied the PM process to produce Nb-V micro-alloyed steel in a study. The work shows that the researchers added V and Nb elements to steel.

Furthermore, they studied how sintering temperature affects the PM steel's microstructure and mechanical properties. They declared 1350°C as the best sintering temperature[3]. Additionally, the authors determined that Nb-V bearing increased the PM steel's mechanical properties, including yield and tensile strengths and hardness. When Nb-V content is added, elongation tends to improve. Moreover, grain growth became limited by Nb-V during the automatization process.

Normally, up to 0.20% by weight of elements like titanium, vanadium, and aluminum can be found in microalloyed steels. These steels belong to a class of materials that exhibit remarkable qualities such good weldability, durability, toughness, and corrosion resistance, because of a variety of processes used for enhancing strength [4].

Powder metallurgy (PM) is described as a procedure that is more beneficial and cost-effective than other production techniques for generating small, useful, difficult-to-manufacture, and incompatible parts, such as high-strength composite structures. Consequently, PM is employed in the production of several mechanical components used in defense, automotive, energy, and medical equipment.

Nickel functions as an austenite stabilizer in steel, causing the ferrite zone to shrink and the austenite region to enlarge. Nickel increases its ability to resist oxidation and corrosion at high temperatures. Its hardness and strength are increased through a process called grain size refinement. It prevents unnecessary growths on the surface. It enhances critical cooling rate, ductility, hardness, and fatigue resistance when coupled with chromium. Elemental nickel diffuses into iron more slowly than many other elements because it has a lower diffusion coefficient, another important thing is the relationship between the PM steel manufacturing, its mechanical characteristics, corrosion behaviors, and microstructure. They have been the subject of extensive research in the fields of materials science, mechanical engineering, and metallurgy. Microalloyed Nb-V PM steel was developed by Erden, investigated how sintering temperature affects the hardness and tensile characteristics of PM steel. His findings show that 1350 °C is an ideal sintering temperature. The author also found that the hardness and strength of PM steels were improved by adding Nb-V to steel. The impact of TiN addition on tensile strength of PM steels was examined by Turkmen et al. [8].

The findings demonstrated that 0.1, 0.2, or 0.5 percent additions of TiN improve the tensile strength of powdered metal [5].

Cr-Ni steel was produced using the PM process by Demirtaş and Erden. This study investigated the impact of Cr-Ni addition on the tensile strength of plain carbon steel. In order to do this, Cr-Ni (0.5-3wt %) was added to the matrix that contained 0.5 C using the PM process. Investigating the impact of Cr-Ni addition on the tensile behavior involved conducting the tensile test, measuring the microhardness of the material, and analyzing its microstructure. This led to the discovery that adding alloying elements boosted mechanical qualities, but the mechanical properties deteriorated as alloying element levels exceeded 1wt%.

Wang et al. produced 35CrMo high-strength steel matrix that was strengthened with TiC reinforcement (50wt %) using traditional powder metallurgy (PM). The findings indicated that the optimal heat treatment procedures for the composite are annealing at 850°C for half hour, quenching at 880°C for half hour, and tempering at 560°C for an hour.

When WC-10AISI304 hard metals were sintered using a pseudo-hot isostatic pressing technique in vacuum at 1300°C and at 20MPa pressure, Trung et al. looked into how NbC affects densification, grain development, and other parameters. In order to lessen the occurrence of g-phase (M6C or Fe3W3C) during the sintering process when 1, 1.5, 2, or 5wt% NbC was added to WC-10AISI304 powder mixture when 2wt% graphite was already added. A high NbC concentration (5wt %) increased the development of coarse grains of (Nb, W) C, which lowered the hardness, according to an elemental analysis. By promoting hard metal grain refinement and restricting the development of g-phase during sintering, the 2% NbC addition produced the maximum Vickers hardness and moderate fracture toughness.

While investigating the effects of Ni addition on the wear and corrosion properties of Nb-V PM steel, this study is mainly focused on how changing the content of Nb, V, and Ni affects the microstructure Corrosion and wears patterns.

The benefits of adding Ni on the steel corrosion and mechanical properties of steels have been documented. Still, a few previous studies have shed light on how Ni affects the Fe-C-NbV micro-alloyed steel composition, which was produced using powder metallurgy (PM). PM is a very important production process for producing different forms of steel. PM steels containing Ni will be required in the future for production without machining, net shape production, or improving the steel corrosion and mechanical properties. This study has been conducted with a main objective of understanding the effect of adding Ni up to 40wt% to the alloy (Fe-C-NbV) and testing corrosion, mechanical properties, and steel microstructure [4].

1.1 PURPOSE OF THE STUDY

The main purpose in this work is to produce alloy of steel with nine different compositions by adding graphite, Nb, V and Ni in different proportions into Fe powders. Characterization of alloy steel samples containing different amounts of Nickel will be examined by applying corrosion test, wear test, hardness test, optical microscope, XRD, SEM Mapping and SEM EDS analyses.

PART 2

LITERATURE REVIEW

Experts have defined powder metallurgy (PM) as a beneficial economic production process to manufacture hard-to-produce components (functional, small, composite, and compatible structures) with minimum tolerance, high strength, and minimum wastage. Basically, powder metallurgy technology transforms different powders into useful engineering substances after a few processes. Recently, some automotive components have been completely produced using powder metallurgy technology.

In fact, powder metallurgy is a novel and unique production process because of its controllable content, homogenous distribution, low cost, and high-quality results. Moreover, it allows the ability to control the forms and sizes of the produced steels, which helps determine the formation temperatures and the exact dissolution. When the best sintering environment is determined, it helps the steel's required perlite and ferrite formation. aircraft parts, automobile spare parts, electrical connection components, nuclear power plants, high-temperature filters, armor-piercing materials, clock parts, orthopedic materials, high-power lighting, and jet engines require production procedures through powder metallurgy [5].

In recent years, a significant proportion of alloyed steels have been produced as tube and flat products. For forging purposes, the production of alloyed steels has gained momentum. Now, micro-alloyed steels are produced using the PM, but its production is insufficient.

Many studies highlight the relationship between Ni and PM steel production, microstructure, and mechanical properties. The optimum weight percentage of nickel consumed to form an alloy is 1.5-2%, and the sintering temperature is 900-1000°C for nickel used in appliances for daily usage. The mentioned work clearly indicates the

effect of adding nickel on the alloy's mechanical properties. Both the samples showed high hardness values, which were suitable for applications including corrosion-resistant marine appliances and shafts.

According to Erden et al, based on the investigated the friction-wear efficicncy of the alloying element in NB-Al microalloy steel by adding 0.1-0.15-0.2% by weight of Nb-Al powder to the matrix. On the other hand unalloyed steel had the lowest wear resistance, alloy with 2% Nb-Al added the best results in terms of wear resistance [6,7].

Moreover, According to Tracey and Upadyaya's studies, the elemental nickel diffuses into iron relatively slowly that because it has a poor diffusion coefficient when compared to several other elements, for example carbon, copper, and molybdenum. This resulted in insufficient dispersion during the sintering process [8].

According to H. A. Raghs, et al, during the corrosive wear fluid arriving the wear zone removes the heat from the wear environment that will lead to the abrasive wear behavior takes place in a more controlled manner. As a result, the quality of the material surface increases [9].

This study, however, examines the effects of adding Nb-V on the mechanical as well as microstructural properties of Ni PM Steel. It specifically focuses on additions of Nb, V, and Ni contents and their impact on Microstructure, Wear and Corrosion Behaviors of Micro alloyed Steels Produced by Powder Metallurgy.

PART 3

MICROALLOY STEELS

A micro alloy steel is a steel alloy with a very small percentage of alloying elements (0.05-0.15%), and the alloying substances include vanadium, niobium, molybdenum, titanium, boron, zirconium, and rare-earth metals. The reason behind their application is: They help facilitate precipitation hardening and refine the grain microstructure.

3.1. DEFINITION OF MICROALLOY STEELS

A major reason behind developing micro alloyed steels was developing good mechanical properties (mainly toughness and strength) that help reduce the required amount of material, specifically for reducing weight in some applications, and better mechanical properties. Micro alloyed steel contains trace amounts of alloying metals like zirconium, vanadium, niobium, molybdenum, titanium, and rare earth elements. They aid in the grain microstructures' refinement. Micro alloyed steels perform between low-alloy steel and carbon steel in terms of price and performance. Without any heat treatment, its yield strength ranges widely (275-750MPa or 40-110ksi). They offer good Weldability, which can be further enhanced by lowering the carbon concentration, and strength is not lost. When compared to other heat-treated steels, their wear resistance and fatigue life are superior. The main drawbacks of these steels are their lack of ductility and toughness. Because the material needs to be cooled quickly to 540-600°C (1004-1112°F) after forming, all the alloys that are present in the solution must be adequately heated. Most cold-worked micro alloyed steels often require less cold working than carbon steels to obtain the same strength, which increases ductility. After the air-cooled state, the majority of hot-worked microalloyed steels are useful. When subjected to control cooling, the material exhibits good mechanical qualities that are almost identical to those of Q&T steels. They nonetheless

have higher machinability compared to Q&T steels because of their hardness and ferrite-pearlite microstructures [10].

It is a fact that because micro alloyed steels do not have a softer and tougher core, which is why they do not need straightening or stress relief. They are also not prone to quench cracking.

3.2. DEVELOPMENT OF MICROALLOY STEELS

Micro alloyed steels have been developed during the last 50 years. Their initial development was limited to just niobium addition. In a 1959 research report by Beiser, the phrase “micro alloy” was first used in reference to steel. It revealed some observations following minor additions of niobium to steel after industrial heating of carbon steel. However, it was not recognized back then as a micro-alloying technique, which had only been discovered 35 years ago when carbon steels were given minuscule zirconium additions. Researchers like Field and Beckett reported their findings. Zirconium steel was developed as a result of the requirement for military equipment. The US War Industries Board started an extensive experimental program to develop huge amounts of zirconium steels, which can be used in light armor, not long after the US entered World War I in 1918. However, it was abandoned after the conflict was over, which caused renewed interest in Q&T steel alloys, which often contain molybdenum, vanadium, and chromium in miniscule amounts (0.5–3%).

Between 1955 and 1960, a significant portion of the earlier work—which was focused on niobium MA steels-reemerged, but it was mostly concentrated in the UK and the USA. The development of micro alloyed steels received substantial support from the British Iron and Steel Association in Sheffield, Sweden Labs of the United Steel Corporation in the vicinity of Rotterdam, and the University of Sheffield. Morrison and Woodhead's thorough documentation and study of the steel's development history was crucial in illuminating the behavior of niobium carbide in ferrite grain refining and dispersion strengthening, both of which led to the increased strength in mild steels. His work's first sentence has been cited as follows: The Great Lakes Steel Corporation, a branch of the US National Steel Corporation, developed its GLX-W series of

niobium-treated steels in 1958, making it unquestionably the first steel company to do so in the history of the steel industry, as it was reported in the Journal of Metals at the time. A very little and inexpensive addition of niobium (0.005-0.03%) made this invention unique by producing a sizable strengthening effect and a high level of toughness. Additionally, niobium addition to semi-killed C-Mn steel (mild steel) changed its strength from low-yield (almost 300MPa) to high-yield strength (415MPa) for grade GLX-60-W, equivalent to the yield strength of traditional alloy steels. According to the manufacturing history of steel, certain significant advancements were successful as a result of the concurrent developments. The Great Lakes Steel Corporation did so as the publications by Hall, Petch, and Cottrell show, which gave rise to a real-time understanding of some of the elements that affect toughness as well as strength. The lower yield stress, sometimes referred to as the 0.2% proof stress, and its relationship to the ferrite grain size are both easily accommodated by the Hall-Petch equation in this context by the variable[11].Furthermore, the experimental constants ky and o are represented. The Hall-Petch equation given above served as the foundation for evaluating the strengthening components, which will be covered later [13].

Precipitation of Q&T steels became an important focus of the initial studies because of the introduction of Siemens' Elmiskop I, a 0.8nm transmission electron microscope (TEM), during the same time period. Electron micrographs had previously been published in a number of US newspapers before that. A high-resolution microscope was available, but despite the fact that many of them were focused on steels, very little thought was given to how to interpret the results. A majority of investigations conducted at that time mostly examined replicas' surfaces. Following Heidenreich's groundbreaking work (1949), Hirsch et al. created thin alloyed foils, including some steels, at Cambridge. The dynamic diffraction contrast and kinetic theories were created over the course of a few years, and they were tested for specific characteristics, which were seen in TEM specimens, such as dislocations, precipitates, and grain boundaries. Another method originally developed for the TEM has been widely applied during the past 20 years. The approach was known as the electron back-scattering diffraction method. Utilizing flexible software, the SEM approach was used to gather details on grains and sub-grains, specifically their borders. The

martensite/austenite phase, which has been a prominent component of contemporary high-strength and tough MA steels, was one of the phases that were tested. The advancement of technology in hot rolling, the primary method of creating MA steels, and steelmaking were some other goals. To guarantee that niobium steels attain their potential properties, new, more stringent methods were required. They required understanding of niobium carbide and nitride solubility. Before beginning the rolling process, it makes sure that the precipitates created during the casting process are added to the solution. In most cases, it entails operating at high temperatures, but that is not a standard procedure. Furthermore, it became clear that the temperatures should be regulated, which led to the development of controlled rolling. Soon after the introduction of computer controls in numerous elements of steelmaking, the outcomes of academic computer modeling were used to support the challenging process of producing small (< 10μm) and homogenous ferrite grains [14].

In Figure 1, the changes over time in properties and microstructure of plate steels have been schematically shown with an alloy design and processing advances. Pipeline steel developments are examples of HSLA steel research (TMCP: thermo mechanical controlled processing; ACC: accelerated cooling; DQ: direct quench).

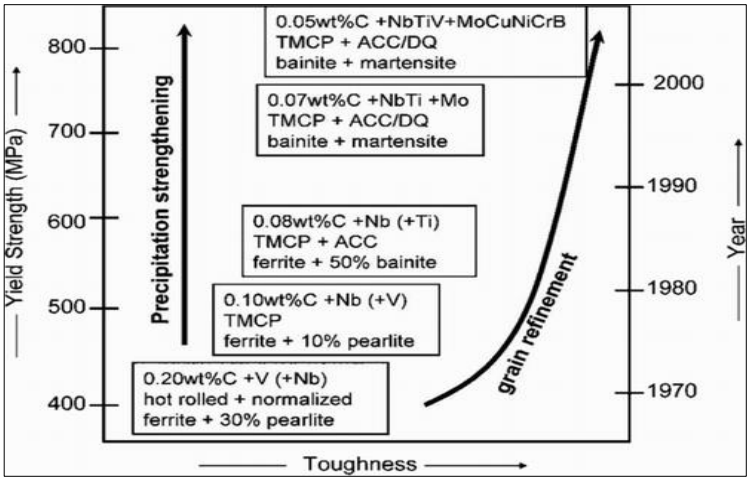

Figure 1. Properties and microstructure changes in plate steels over time [12].

The development of MA steels was initiated in several directions during the early years because of the ongoing quest to produce high-strength structural steels at an affordable price. In most cases, hot rolling was used to clarify the deformation mechanisms and

the function of the microalloying additions. Thermo-mechanical processing, particularly involving microstructure, characteristics, and controlled rolling, has been improved by a greater knowledge of the interrelationships between processing factors. The MA steels involved directly-charged thin slab processing, which is an affordable technique for some goods and has some environmental advantages over conventional procedures. The application of high-strength MA steels in non-FP microstructures (yield strengths y>500 MPa) is suitable for automotive applications. However, friction stir welding (FSW) reduces residual stresses experienced during fusion welding operations at an earlier stage of commercial utilization when used in MA steels. Then, the strength contributions of the nano precipitates were studied. In some circumstances, particularly when a microstructure is summarized, it could change. This thesis is an updated version because it includes hot working process modeling of MA steels. Despite 130,000 Google results for microalloyed steels, the reviews that are accessible are inevitably biased, even though, they are based on reputed works the author has examined over time. Because of their innovative contributions to the findings of numerous international research organizations, some current research articles were also consulted [15].

3.3. PRODUCTION PROCESSES OF MICROALLOY STEELS AND STAGES

Since steel is a primary building material, Bessemer's development in 1856 can be directly attributed to it. When molten pig iron is blown in a converter using a compressed air stream, it melts a large bulk of iron. The steel scrap, which may come from outdated fixtures, buildings, or equipment or it may come from technical wastes, accumulates over time, so experts created new steel smelting techniques because of the iron ore’s resource depletion and low P and S impurity concentrations. Martin created the open-hearth technique, also known as the Siemens-Martin process, for the first time in 1865. When a large amount of fuel is utilized, which is necessary to melt the charge and maintain a course of reaction between the combustion gases directed onto its mirror and the molten metal with slag, it involves steel smelting from pig iron and steel scrap in an open-flame-fired furnace. Because Thomas used base refractory materials for the slag-forming and furnace lining, he invented the converter steel that

smelted from pig iron with high P concentration in 1877. Steel smelts with varied degrees of reduction were frequently utilized in these operations for riveted constructions. Thermite and combustible gas interactions generated heat in the final years of the nineteenth century, which was intended to be used for welding steel pieces together. Bonding had been in use for a while throughout those years. Manufacturing costs can be brought down, but that depends on welding technology. The technology of electrical welding underwent significant improvements at the start of the 20th Century. However, the steel produced at the time frequently caused welded constructions to collapse. During World War II, there were numerous disastrous and problematic failures. When welding was utilized, it resulted in significant material losses and casualties, which created the need for extensive steel examinations and finding the reasons behind the disasters [16].

Further investigation reveals that constructional steels are susceptible to failure or cracking after reaching a particular critical point. They exhibited ductile behavior because they fractured after a significant plastic strain. The crack started at the slightest plastic tension below that point. Tpk temperature increases negatively with increases in O, N, H, and P concentrations since it is not merely a material constant. The same thing occurs when steel's Cr, Si, and C concentrations rise; C is known to be the primary component that strengthens steel products. S has a negligible impact on Tpk, whereas Ni and Mn, in concentrations up to 2%, have an opposite effect. Steel becomes hot-shorted as a result of the iron in FeS, while metallic MnS precipitates with the steel's manganese content. Because of the anisotropy of the plastic characteristics in flat goods, it is subjected to plastic strain at a high temperature, which reduces the weldability of steel. Low metallurgic steel purity was the cause behind frequent catastrophes, according to the results of the investigation. The development of nitriding in the welds and heat-affected zone, the possibility of oxidation, and the development of coarse-grained structure in the welded joints were all caused by increased P, S, and N concentrations, a high percentage of the used auxiliary materials, unfavorable welding conditions, and deformable non-metallic inclusions. The oxygen-blown converter, which was created in the 1950s, and electric arc furnaces, used for alloy steel smelting, led to metallurgic purity of steel. Smelting construction steels in electric furnaces has become more significant for environmental reasons. Later studies

found, and the Hall-Petch connection has validated that the value of y (lower yield point limit) of the polycrystalline iron increases with decreasing average grain size [17].

The following list includes various micro-alloyed ferrite pearlite steels.

- Micro alloyed steels with niobium
- Micro alloyed steels with vanadium
- Steels with micro alloyed vanadium-niobium
- Steels with micro alloyed vanadium-nitrogen.
- Steels made of titanium micro alloyed, vanadium-titanium micro alloyed, and niobium-titanium micro alloyed sets.

3.3.1. Flat Products

3.3.1.1. Austenitization (Solution annealing)

Austenite is essential for the production of steel, and the austenite condition that develops during processing is managed to optimize the resulting microstructure. It is a fact that no perfect austenitic microstructure exists for any application, despite improvements in the automatization heat treatments over decades. It is often advantageous to reduce austenite grain formation during processing, and it should be made sure that the alloy composition is as homogenous as possible in the microstructure. Controlling microalloying, thermo-mechanical techniques, or processing temperatures can prevent grain development. For high-heat processes (like surface induction hardening), austenite composition and homogeneity should be carefully considered because that is important for the development of low-carbon AHSS sheets, which need understanding of local phase stability and precise processing paths.

In some alloy systems, many processing opportunities are not available. They are still accessible in this system, making steel the most important structural material in use today. It has consistently led to significant breakthroughs in steel applications for more than a century. The current trend is anticipated to continue in the near future, based on

a few recent advances in the theoretical understanding of steels and process capabilities [18].

3.3.1.2. Controlled Rolling and Controlled Cooling

Controlled rolling can enhance steel characteristics to a point where they match with highly alloyed or heat-treated steels. A high temperature deformation of the re-crystallization region, a low temperature deformation of the no-recrystallization region (above Ar3), and a third deformation of the austenite-ferrite region are the three stages of controlled rolling. In the zone with no recrystallization, the deformation process is crucial. Its importance is dependent on the austenite grain partition into several blocks, which is a consequence of adding deformation bands to the grains. After transformation, deformation creates a composite structure in the austenite-ferrite zone with corresponding grains and sub-grains, further boosting the material's toughness and strength. Ferrite nucleation, which only happens at austenite grain boundaries in hot-rolled steels, is a fundamental difference between traditionally controlled-rolled and hot-rolled steels. In the former, it happens at grain boundaries in the inner grains, resulting in a more refined grain structure.

Fig 2 shows the process, through which we have divided the controlled-rolling process into three temperature regions, including the austenite non-recrystallization region, two-phase austenite-plus-ferrite region, and austenite recrystallization region. Using a constant slab-to-plate reduction, as the schematic figure shows, the microstructures of austenite grains during rolling and ferrite grains are drawn for the following three kinds of rolling of the final plates after air cooling: (i) traditional finish-rolling in the recrystallization region above 900°C, (ii) light controlled-rolling that consists of a cumulative reduction in non-recrystallization and recrystallization regions and (iii) severe controlled-rolling that consists of a cumulative reduction in all three regions. As the finishing temperature is lowered compared with the conventional rolling temperature, ferrite grains in the rolled plate become finer [19].

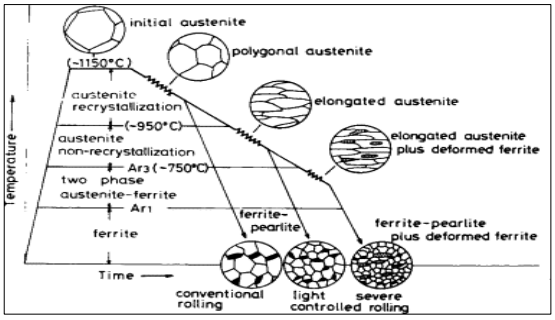

Figure 2. Schematic comparison between the controlled-rolling process and conventional rolling and resultant microstructures for niobium-bearing steel [20].

Moreover, the mechanical properties and microstructure can be improved after finishing rolling through rolling speed, controlled rolling temperature, and cooling speed. As a consequence, normalizing and other sequential heat treatments can be eliminated. Experiments were conducted on the cooling of bars, and controlled rolling was carried out using different control technologies in the bar mill, which was constructed to reproduce preceding heat patterns. The heat patterns of rolling resulted in certain microstructures, which emerged by controlled rolling and cooling.The outcomes of the experiments were as follows: To obtain finer-grained structured steel, the finishing rolling temperature was controlled below 900°C using intermediate cooling. After rolling, powerful cooling made it possible to quench bars with a bainite structure in the core in the actual bar mill line and the martensitic structure on the surface [20].

3.3.2. Micro-alloy Tube Steels

This type of steel is an alloy steel with alloying elements in extremely little quantities (0.05–0.15%). They include zirconium, niobium, vanadium, titanium, boron, and molybdenum. They helped precipitation harden while also enhancing grain microstructure.

Microalloyed steels often fall between low alloy steel and carbon steel in terms of price and performance. Without any heat treatment, their yield strength range is 275-750MPa (40-110ksi). Although their Weldability is normally good, it can be further enhanced by reducing carbon while keeping strength at the same time. For comparable

heat-treated steels, wear resistance and fatigue life are superior, but they have drawbacks. Their ductility and hardness, for instance, are inferior to those of Q&T steels. They are heated sufficiently to create any of the alloys in order to dissolve them into the solution, but once formed, they must be rapidly cooled to 540–600°C (1004–1112°F) [21].

Cold-worked micro alloyed steels are more ductile because they require less cold work to gain a similar strength as conventional carbon steel. In the air-cooled state, hot-worked micro alloyed steels are employed. When controlled cooling is applied, the material's mechanical characteristics become just like those of Q&T steel, primarily because of their ferrite-pearlite microstructures and more uniform hardness, they are more machinable than Q&T steels.

Micro alloyed steels are normally through-hardened, but unlike Q&T steels, they do not have a tougher and softer core since they are not quenched or tempered, making them resistant to quench cracking and not needing to be stress relieved or straightened [22].

To assure strength just like other carbon steels, cold-worked micro-alloyed steels do not need significant cold working, which leads to greater ductility. In the air-cooled state, hot-worked micro alloyed steel is used. In the case of controlled cooling, the material produces mechanical characteristics like the Q&T steels. As compared to Q&T steels, their machinability is more because of their ferrite-pearlite microstructures and more uniform hardness. Since micro alloyed steels are neither tempered nor quenched, they are unsusceptible to quench cracking [14].

3.3.3. Forged Products

They are materials resulting from carbon and alloying iron under extreme pressure. Steel becomes ductile and malleable when it gets heated to a forging temperature,

which makes it possible to mold it into the required shape by applying pressure and force [24].

3.3.3.1. Machinability of Microalloyed Forged Steels

The machinability of Q&T steels (AISI 1045 and 5140) and micro alloyed steel (30MnVS6) in various cutting situations has been mentioned by a few researchers. An experimental examination was conducted to ascertain the impacts of a workpiece material's feed rate, cutting speed, and hardness, on the coated and cemented carbide inserts' tool life as well as the flank wear land during the hard turning process. The hardness levels of the steel were tested under various test scenarios until they nearly matched, which was made feasible by utilizing the proper heat treatments. A statistical analysis was done to determine the impact of various variables on cutting forces. The length of the tool contact was examined with chip properties. Using a scanning electron microscope (SEM), various portions of the chip (including the microcrack, shear plane, edge, and thickness) were studied. Microcracks and shear planes in the steel chips made of micro alloyed alloy display predictable and erratic patterns. A video microscope was used to observe the crater wear on the tools as they were turned. The results show that, under identical cutting conditions, the micro alloyed steel has a comparative advantage over QT steels in terms of machinability and tool life [24].

3.4. MICROALLOY ELEMENTS

3.4.1. Titanium (Ti)

Titanium, written as Ti, has atomic number 22 and weight 47.867 (measured in Daltons) in the periodic table. This beautiful transitional metal has a high strength, low density, silver color, and resistance to corrosion in seawater, chlorine, and freshwater.

William Gregor discovered it in 1791 in Cornwall, England, and Martin Heinrich Klaproth named it after the Titans of Greek mythology. Because of its presence in many mineral formations, primarily rutile and limonite, it cannot be considered an independently occurring element. Since they are dispersed across the whole

lithosphere and crust of the Earth, they can be found in almost every living creature as well as in rocks, soils, and water. The Kroll and Hunter procedures are used to separate the metal from its main mineral ores. The most prevalent substance, titanium dioxide, is utilized in the production of white pigments as a well-liked photocatalyst. Other substances that contain it are titanium trichloride ($TiCl_3$) that catalyzes polypropylene during manufacturing and titanium tetrachloride ($TiCl_4$), a component of smoke screens [2].

The aerospace (missiles, spacecraft, and jet engines), desalination plants, petrochemicals, chemicals, paper, and pulp), agricultural (farming), medical prostheses, automotive industries, orthopedic implants, dental implants and instruments, jewelry, mobile phones, and sporting goods are just a few applications for which this metal can be alloyed.

The two most advantageous characteristics of the metal, which are also the highest for any metallic substance, are its strength-to-density ratio and corrosion resistance. In unalloyed condition, titanium is less-denser but as stronger as some steels. This element occurs in five naturally occurring isotopes, ranging in abundance from 46Ti to 50Ti (48Ti being the most prevalent at 73.8%), as well as a few allotropic forms [12]. Despite belonging to the same group, and having the same amount of valence electrons, zirconium and titanium exhibit numerous different chemical and physical characteristics.

Figure 3. Titanium (Ti) [15].

3.4.2. Vanadium (V)

Its atomic number is 23 and Periodic Table symbol is V. It is often a hard, silvery-grey malleable metal. This elemental metal is uncommon, but after being artificially isolated, the oxide layer formation partially stabilizes it against oxidation.

Vanadium was first identified as “a novel lead-bearing mineral” by Andrés Manuel del Rio in 1801, and it was later referred to as "brown lead" after further examination. This discovery was made in Mexico. He initially believed that the characteristics of the newly discovered mineral were because of the inclusion of a new element in it. Later, he was misled into believing that chromium was a typical element in those days by a French chemist named Hippolyta Victor Collet-Descotils. Later, in the 1830s, another scientist named Nils Gabriel Edstrom synthesized various vanadium chlorides, demonstrating that it was a novel element. He gave it the name "vanadium," after the name of a Scandinavian goddess Vanadic (Freyja). The variety of colors present in various vanadium compounds is what gave rise to this name. Vanadinite was the name given to the lead mineral discovered by Del Rio because it contained vanadium. In 1867, Henry Enfield Roscoe discovered vanadium in its pure elemental form for the first time [27].

Vanadium can be found in ores of roughly 65 different minerals and fossil fuel deposits in nature. It is made from steel slag in Russia and China, while it is made directly from magnetite, uranium byproducts, or oil fields in other nations. Its primary use is in the manufacturing of specialized steel alloys, particularly some aluminum alloys and high-speed tool steels.

Vanadium ions, which may be poisons, are present in significant concentrations in a few organisms. Vanadium oxide and other vanadium salts have a moderate level of toxicity. Vanadium is used by a variety of marine life forms as an enzyme active center; for instance, certain ocean algae use vanadium Bromo peroxidases [15].

3.4.3. Aluminum (Al)

Aluminum (or aluminum in Canadian and American versions of English) is a metal represented by the symbol Al in the Periodic Table. Its atomic number is 13.

Aluminum's density is substantially lower than other common metals, roughly one-third of steel. When exposed to air, it forms a protective oxide layer on the surface because of having an affinity towards oxygen. Normally, aluminum looks like silver because of its remarkable color. It is ductile, non-magnetic, and soft. A stable isotope of aluminum is Al_{27}, which is very common and makes aluminum the universe's 12th most common element. Aluminum is a chemically weak metal belonging to the boron group, so just like other group metals, aluminum compounds form in the +3-oxidation state. The highly-charged aluminum (Al_3+) polarizes and forms covalent bonds with aluminum in different compounds. In nature, aluminum has a strong affinity towards oxygen that transforms aluminum into oxides; therefore, aluminum is primarily found in rocks in the crust. That is why, it is abundant, but it seldom exists as a free metal [16].

In 1825, a Danish physicist Hans Christian Orsted announced the aluminum discovery, while French chemist Henri Étienne initiated the first industrial aluminum production in 1856. A French engineer Paul Héroult and a US engineer Charles Martin Hall created the Hall–Héroult process, after which, Aluminum became available to the public in 1886, which led to its mass production and utilization in everyday life. Aluminum was used as a crucial strategic resource in wars and aviation. Aluminum surpassed copper in 1954, becoming the most-produced metal after iron. The 21st Century witnessed aluminum consumption in engineering, packaging, transportation, and construction in Western Europe, Japan, and the United States, Despite the fact that it exists commonly, no organism metabolically consumes aluminum salts; however, plants and animals can tolerate it. Because such salts are abundant, studies are continued on them because they may have a potential for biological use in the future [16].

3.4.4. Niobium (Nb)

Another metal called Niobium (also called columbium) has atomic number 41 and the symbol Nb (previously Cb). It is a crystalline, ductile, and light grey transition metal. On a Mohs hardness scale, its rating is just like titanium, and has same ductility as iron, so it is used in jewelry. It was called columbium because it is often found in

columbite and pyrochlore minerals. This name originated in Greek mythology, in which Niobic was Tantalus' daughter. This name shows great physical and chemical similarities between the two elements, which makes them difficult to distinguish [29].

Charles Hatchet, an English chemist, reported in 1801 that columbium, a new element was discovered and William Hyde Wollaston, another English chemist (1809) thought that it was identical to tantalum. In 1846, German chemist Heinrich Rose found that tantalum ores contain niobium, which is a separate element. A series of scientific findings in 1864 and 1865 clarified that both columbium and niobium were the names of the same element. In 1949, Niobium became the officially-adopted name of the element; however, columbium remained in the US metallurgy circles. Niobium could not be commercially used until the early 20th Century. Brazil is a leading niobium and Ferro niobium producer. Ferro niobium consists of 60–70% niobium-iron alloy. Since then, niobium has been mostly used in alloys and special steels used to manufacture gas pipelines. The mentioned alloys only contain 0.1% niobium, but it significantly improves the strength of steel. For using it in jet and rocket engines, the niobium-containing super alloy's temperature stability must be considered, in various superconductors, Niobium is commonly used. Some superconductor alloys contain tin and titanium, which are commonly used to manufacture MRI scanners' superconducting magnets. Other applications of niobium are in welding, nuclear industries, electronics, jewelry, optics, and numismatics. The last two applications have iridescence produced by anodization and low toxicity, which are highly desired. Moreover, niobium is a technology-critical element [29].

Figure 4. Niobium (Nb) [29].

3.4.5. Carbon (C)

Carbon is taken from Latin. In Latin, it is called carbo or "coal," a chemical element whose atomic number is six, and C is its symbol. It is tetravalent (four electrons are available for covalent bonds) and non-metallic. It can be seen Group 14 (Periodic Table). Only 0.025% of the crust contains carbon. Its three naturally occurring isotopes are 12C, 13C, and 14C, the last of which decays after 5,730 years. Since ancient times, people have been aware of the existence of carbon [30].

Carbon is the most abundant after helium, oxygen, and hydrogen in the cosmos, and 15th most common element in the Earth's crust. Because of its abundance and distinctive diversity of organic compounds, as well as its uncommon capacity to form polymers at ordinary temperatures, carbon is able to benefit both humans and other species on the planet. Its abundance in the human body is second only to oxygen in terms of mass (nearly 18.5%) [30].

When the carbon atoms interact, different carbon allotropes form. Graphite, fullerenes, diamond, and amorphous carbon are the common allotropes of carbon. Different physical characteristics distinguish the various allotropic forms of carbon. Graphite is another type of carbon that is soft, and leaves streaks on paper. The materials with the highest thermal conductivity are carbon nanotubes, graphene, and diamonds. All carbon allotropes are solids but chemically inert at ambient temperature and need a high temperature to interact with other elements, including oxygen [18].

Only a small portion of all compounds that could theoretically exist under typical conditions-approximately ten million compounds have been filed so far. Because of this, carbon is frequently termed the “king of the elements”.

Figure 5. Carbon (C) [18].

3.4.6. Nitrogen (N)

Its symbol is N, and atomic number is 7. First isolated and discovered by a Scottish physician Daniel Rutherford, nitrogen was recognized as an independent element in 1772. At almost the same time, Henry Cavendish and Carl Wilhelm Scheele discovered it, but generally, Rutherford is given the credit because he published his findings before everyone else. Nitrogen is the smallest element in Group 15, often known as the pnictogens. Under normal conditions of pressure and temperature, two atoms combine to form nitrogen. It is a diatomic gas known as N_2 (Dinitrogen), which makes it the most common uncombined element. It is a colorless and odorless gas. All animals' bodies contain it, specifically in the amino acids, proteins, and energy-transfer molecule adenosine triphosphate as well as the nucleic acids (RNA and DNA). After hydrogen, oxygen, and carbon, nitrogen is the fourth most common element in a typical human body, making up 3% of its mass. The nitrogen cycle transfers airborne elements into organic compounds and the biosphere before returning them to the atmosphere [19].

Nitrogen is a component of several significant industrial substances, including ammonia, nitric acid, cyanides, and organic nitrates (explosives and propellants). In elemental nitrogen, which dominates nitrogen chemistry, an extraordinarily powerful triple bond (NN) is the second-strongest bond after carbon monoxide (CO). In order to release significant amounts of useful energy, nitrogen molecules must explode, decompose, or burn, which is difficult for industry and organisms to do. Synthetic nitrates and ammonia are significant industrial fertilizers because fertilizer nitrates are the principal pollutants in different water systems.

In addition to usage in fertilizers and energy storage, it is used in Kevlar, a high-strength fabric, cyanoacrylate to make superglue, and antibiotics. Numerous medications imitate nitrogen-containing signal molecules are found in nature. For instance, organic nitrates that convert into nitric oxide, such as nitroprusside and nitroglycerin, regulate blood pressure. Natural caffeine, manufactured amphetamines, and morphine all work on animal neurotransmitter receptors and are common nitrogen-containing medications [19].

Figure 6. Nitrogen (N) [19].

3.4.7. Silicon (Si)

It is another important element, its symbol is Si, it is a blue-grey brittle solid and its atomic number is 14. The Periodic Table's Group 14 includes it where Carbon is above and tin, germanium, flerovium, and lead are below it. Its affinity with oxygen is strong. Jöns Jakob Berzelius prepared and described it in its purest form in 1823. It is comparatively inert, although it reacts with silicates to form oxides. The melting and boiling temperatures are respectively 3265°C and 1414°C. Despite abundance, it is rarely found in a pure form. It is widely dispersed in space in a variety of forms, such as silicates or silicon dioxide, in planets, planetoids, and cosmic dust (silica). Silicate minerals comprise 90% of the crust, making them the second most common element after oxygen. In the waters of the planet, silicon has existed as a natural element for nearly 400 years [20].

Mostly, natural minerals are processed very little and without separation to produce silicon for commercial usage. It includes silica sand, stone, and clay. Silicates are mostly utilized in Portland cement's mortar and stucco. To form concrete for walkways, roads, and foundations, they are combined with gravel and silica sand. Additionally, they are employed in white ware ceramics, such as porcelain and other specialized glassware as well as conventional soda-lime glass with a silicate base. Abrasive materials and parts of high-strength ceramics are made from some silicon compounds, like silicon carbide. Silicone serves as the foundation for silicones, which are frequently-used synthetic polymers.

The term “Silicon Age” describes the late 20th and early 21st centuries because elemental silicon had a significant economic impact because it is used in transistors and integrated circuit chips. Just a limited amount of pure elemental silicon is utilized in semiconductor electronics (10%), (computers and cell phones). The metal-oxide semiconductor field-effect transistor (MOSFET), produced in huge numbers, is a silicon device that is often utilized. Free silicon has also been employed in the fine chemical, aluminum casting, and steel refining sectors (to make fumed silica) [20]. In biology, silicon is a crucial element, yet animals only need traces of it. However, silica is a component of many microbes and marine sponges, including radiolarian, diatoms, and skeletal structures. It accumulates in numerous plant tissues [20].

Figure 7. Silicon (Si) [20].

3.4.8. Phosphorus (P)

Phosphorous is another chemical element that is placed second in the group of agonists in the Periodic Table and is one of the antigens. Phosphorous is a non-metal, and it is freely available in several forms (or allotropic forms). White and red phosphorous are the most famous forms. The phosphorous concentration in the earth's crust reaches almost 1g/kg in the phosphate form. For the first time, it was isolated in 1669 in white phosphoric form, and when exposed to oxygen, it emits a faint flicker, which is a poison, and received this name from Greek Φωσφόρος (phosphorus); means light like a morning star, which also means Venus. Phosphorous enters into the synthesis of phosphate 3-PO_4; it is an essential element for life and can probably be the main body of RNA, DNA, instant lipids, and adenosine triphosphate (ATP). In some aquatic organisms, its concentrates are the root for growth and are also a part of the oceans and mantle. It is mainly obtained from phosphate-containing minerals, which are

extensively used in manufacturing detergents, fertilizers, and pesticides, to mention a few [21].

3.4.9. Manganese (Mn)

The symbol of manganese is Mn, and its atomic number is 25. It is often found in combination with iron in a brittle silvery metal form. Manganese has several industrial uses, specifically in stainless steel. It improves the workability, resistance to wear, and strength of tools. Normally manganese oxide is used as a rubber additive and an oxidizing agent for making fertilizers, ceramics, and glass. Another compound, manganese sulfate, is used as a fungicide [22].

It is surprising for many people that manganese is also an essential human dietary element, and it is very important for bone formation, macronutrient metabolism, and defense against free radicals. In dozens of enzymes and proteins, it is a critical component [3]. It mostly exists in the bones, but to some extent, it is also found in the kidneys, brain, and liver. Manganese in the human brain is bound to manganese metalloproteinase.

For the first time, it was isolated in 1774. In the laboratory, it is a familiar substance, and it exists in the form of potassium permanganate, a violet salt. In some enzymes, it occurs in the active sites. The scientific community expressed interest in using the Mn-O cluster, which is found when plants produce oxygen [22].

Figure 8. Manganese (Mn) [22].

3.4.10. Nickel (Ni)

Ni is the symbol for this element, and its atomic number is 28. It is a transitional metal, but unlike many others, it is ductile and durable. Pure nickel is converted into a powder

for increasing its reactive surface, which exhibits substantial chemical activity; nevertheless, under normal circumstances, large pieces slowly react with air. It also exists in nickel-iron meteorites, which never exposed to oxygen.

The discovery of meteoric nickel and iron together is intriguing because it sheds light on the genesis of these metals, which are important byproducts of supernova nucleosynthesis. Iron and nickel combine to form the both inner and outer core of the Earth [23].

Nickel usage (meteoric nickel-iron alloy) dates back to 3500 BC. In Sweden's Los Hälsingland cobalt mines, nickel was initially mistaken for a copper mineral deposit when Axel Fredrik Cronstedt isolated and later classified it in 1751. Its name is derived from the naughty sprite-nickel of German mythology, demonstrating that copper-nickel ores could not be refined into copper. A significant economic nickel source is iron ore that contains 1-2 percent nickel. Pentlandite and a naturally occurring silicate combination rich in nickel (garnierite) are other significant ore minerals. One of the main production locations is the meteor-originating Sudbury region of Canada. Additionally, it is discovered in the Pacific and in Russia.

At room temperature, it gradually oxidizes and is considered corrosion-resistant. In the past, it was employed to coat chemistry lab equipment, plate iron and brass, and create certain alloys with a high silvery sheen. German silver is an example. The production of corrosion-resistant nickel plating uses almost 9% of the world's nickel supply. The finished items can occasionally result in a nickel allergy. Nickel has long been a popular metal used to make coins, but as its price has risen, governments have been obliged to switch to more affordable metals [23].

Figure 9. Nickel (Ni) [23].

3.5. EFFECTS OF MICROALLOY PRECISION

3.5.1. Carbide and Nitride Precipitation

The niobium carbonitride precipitation in the interphase, ferrite phase, and austenite phase of micro alloyed steel has been assessed in a critical literature review, and it has been a topic of a round table discussion. The current work analyzes the niobium carbide precipitates' contribution in ferrite for the precipitation hardening process of commercial hot rolled strips. Kinetics and thermodynamics of niobium carbo-nitride precipitation, including the effects of temperature and deformation on the precipitation kinetics, have been discussed with various examples to determine the niobium quantity in a solid solution, which is available for precipitation hardening in the austenite phase after thermo mechanical rolling and successive phase transformations [24].

3.5.2. Effects of Temperature and Cooling Rate on Precipitation

The heating rate affects precipitation before solution treatment. In contrast, the cooling rate affects the morphological distribution and evolution of the nickel-based single-crystal superalloy's precipitation phase after solution treatment. The matrix' precipitation, growth, dissolution, and precipitation phases were analyzed during heat treatment through a high-power scanning electron microscope. According to the results, the precipitated phase morphology has nothing to do with the heating rate in the heating process and precipitated phase distribution; however, the cooling rate during the cooling process affects the size, distribution, and shape of the precipitated phase. If the cooling rate is faster, the precipitated phase will be smaller, and if the shape is irregular, the equivalent edge length and channel width of the matrix phase will be smaller [4].

3.6. STRENGTH-INCREASING MECHANISM IN MICROALLOY STEELS

The overall strength of hot-rolled micro alloyed steels results from a number of concurrently occurring strengthening mechanisms, such as grain size refinement-induced hardening, transformation-induced dislocation strengthening, solid solution-strengthening, and precipitation strengthening. The micro alloyed steels' mechanical properties are improved by precipitation of fine carbonitride particles using thermo-mechanical processing, where small amounts (less than 0.1 weight percent) of strong carbide and nitride forming elements, like niobium, vanadium, and titanium are used for precipitation strengthening and grain-refinement. In micro alloyed steels, the fine carbonitride particle production, which has an average diameter of less than 10 nm, is essential for both precipitation strengthening and grain refining. During final cooling, it can develop in ferrite in the form of semi-coherent particles or in austenite during hot rolling or austenite-to-ferrite transformation. Each of the previously stated primary precipitation modes results in a distinctive particle distribution and various consequences on the characteristics of steel. Early in the 1960s, systematic research on micro alloyed steels was conducted at the University of Sheffield [25].

Which included the first observations of carbonitriding particles made using transmission electron microscopy (TEM). Moreover, the existence of tiny carbonitride particles that can be seen under a TEM is what makes a yield strength contribution of almost 100MNm-2 in a rolled condition. For titanium and niobium/vanadium steels, cases of greater contributions (up to 200 MNm-2) have been documented. In general, the experimental findings support theoretical hypotheses based on the Orowan-Ashby precipitation strengthening model with carbonitride particles having a diameter of 3 nm [26].

3.6.1. Reducing Grain Size

Grain size reduction lowers the total amount of pile-up that might form at the border, which raises the applied stress. In order to shift a potential dislocation across the grain boundary, stress must be applied. Higher yield strength is the result of applying more stress to shift the dislocation [27].

3.6.1.1. Determination of Grain Size

The planar grain size is measured either manually or by image analysis based on their historical development and their relation with basic stereological concepts. The discussed methods include some comparison techniques, which employ the Shepherd fracture grain size standards or the standard charts; determination of the grains per unit area through measurement techniques (Jeffries method), the triple points per unit area, or grains intercepted/grain boundaries intersected per test line's unit length (Heyn method); and the correlations, which are based on grain shape assuming estimated spatial grain size characteristics. Specific procedures are also discussed to measure the grain size of duplex, multiphase, or non-equiaxed grain structures. Such techniques have been mentioned, along with information about the grain size measurement accuracy.

3.6.1.2. Determination of Ferrite and Perlite Ratios

Using electron probe microanalysis and optical microscopy, the alloying elements' microstructure and distribution in a low-alloy hot-rolled steel plate contains 0.26%Si, 0.15%C, 0.03%Al, and l.49%Mn (wt.%). Alternate pro-eutectoid pearlite and ferrite bands were found in the solute-rich and solute-lean zones, respectively, as a result of the micro chemical banding of manganese. Bands were clearly developed at 0.1Ks−1 cooling rate; however, the intensity of the banding process decreased after chilling at 1 K s−1. The production of "slabs" of pro-eutectoid ferrite in manganese-deficient locations led to austenite disintegration, which in turn led to growth of ferrite grains. Abnormally massive austenite grains that crossed many bands were produced as a result of the creation of enormous, irregularly distributed pearlite nodules. Ferrite/pearlite banding was absent in austenite grains areas when the specimens were cooled at 0.1Ks−1 [36].

3.6.2. Precipitation Hardening

Particle hardening and age hardening are other names for it. It is a method of heat treatment for raising the yield strength of malleable materials, such as certain structural

alloys of magnesium, aluminum, titanium, and nickel, as well as some stainless and other steels. Super alloys, which offer great high-temperature strength, have a history of developing anomalies in yield strength [28].

Precipitation hardening is impacted by changes in solid solubility with temperature that results in tiny impure phase particles. It prevents the lattice movement of a crystal of a dislocation or fault. The material hardens as a result of some dislocations acting as the main carriers of plasticity. In particle-reinforced composite materials, the aforementioned contaminants and particle compounds play the exact same roles. Depending on the thermal history of the environment, ice formation in the air can result in snow, hail, or clouds, but precipitation in solids results in a wide range of particle sizes with drastically different properties. In contrast to regular tempering, alloys must be held at high temperatures for a number of hours in order to allow precipitation. A couple of heat treatments involving residues can alter the material strength: Precipitation heat treatments and solution heat treatments. The latter involves a single-phase solid solution formation through quenching the addition of impure particles during precipitation heat treatments to increase a material's strength [29].

3.7. ADVANTAGES OF MICROALLOY STEEL

Low-carbon steels with tiny proportions of alloying elements are known as micro-alloyed steels, or high-strength low-alloy (HSLA) steels, to achieve yield strengths more than 275MPa in the normalized and as-rolled conditions. As compared to as-rolled C steels, this form of steel almost usually has better mechanical qualities and occasionally exhibits greater corrosion resistance. A higher strength of the micro-alloyed steels is feasible with lower C concentrations. Weldability of some micro-alloyed steels is at par with superior to mild steel.

A small amount of micro-alloying components is used in the micro-alloying technology, and they are combined with basic low-C steel. The usage of the micro-alloy concentrations results in remarkably different mechanical characteristics. It makes the alloying technology distinct in the traditional sense (low alloy steel family). The concentration of the alloying components in this instance varies from 0.25% to 1,

2, or even higher percentages. Micro-alloyed steels are specifically created to have superior mechanical qualities and a higher resistance to air corrosion than typical C steels. Since alloy steels are created to satisfy particular mechanical requirements as opposed to concentrating on a particular chemical composition, they have generally not been taken into consideration, Low alloy steels or low or medium carbon steels with added elements such as titanium (Ti), niobium (Nb), zirconium (Zr), and vanadium are known as micro-alloyed steels (V). Both separately and in various combinations, the aforementioned additions increase the strength of the steel. A workpiece can be made more machinable by adding tellurium (Te) and sulphur (S) under regulated conditions. Because of the micro-alloying strengthening components, the C content can be drastically reduced while still greatly increasing notch toughness and Weldability [38].

3.8. APPLICATION AREAS OF MICROALLOY STEELS

High Strength Low Alloy (HSLA) or Micro alloy (MA) steels, which account for over 12% of all steel produced globally, are a significant steel category. They are now utilized in practically all-important steel market sectors throughout the globe. Some industries, like building, transportation, and oil and gas production saw greater expansion as a result of their development. Table 1 lists the definitions of alloy, low, and microalloyed steels.

Table 1. Definitions [30].

Alloy Steel	Steel that contains significant alloying elements like carbon (manganese, silicon, etc. are exceptions) to change mechanical or physical properties.
Low Alloy Steel	Containing 3.5% or less alloying elements in steel, for example, 1% Mo or 2.25% Cr.

Micro Alloy Steel	Steel that contains small quantities of niobium, titanium, or vanadium, each of them is generally less than 0.10%, and the total micro-alloying elements are normally less than 0.15%. They are also termed HSLA steels.

PART 4

POWDER METALLURGY

Modern metal-forming techniques such as powder metallurgy use heat-compacted metal powders until their temperatures are slightly lower than their melting point. This method has been around for almost a century, it has only recently gained widespread acceptance as a great way to produce components of significant applications. Because of the benefits this method has over other metal processing technologies, like metal casting and forging, it is currently a successful and well-liked method. It is advantageous for near-net-shape dimensional control, shape complexity, and material utilization, to name a few. Powder metallurgy, or PM, an actual green technology, significantly contributed to production processes figure 10 demonstrates powder metallurgy stages.

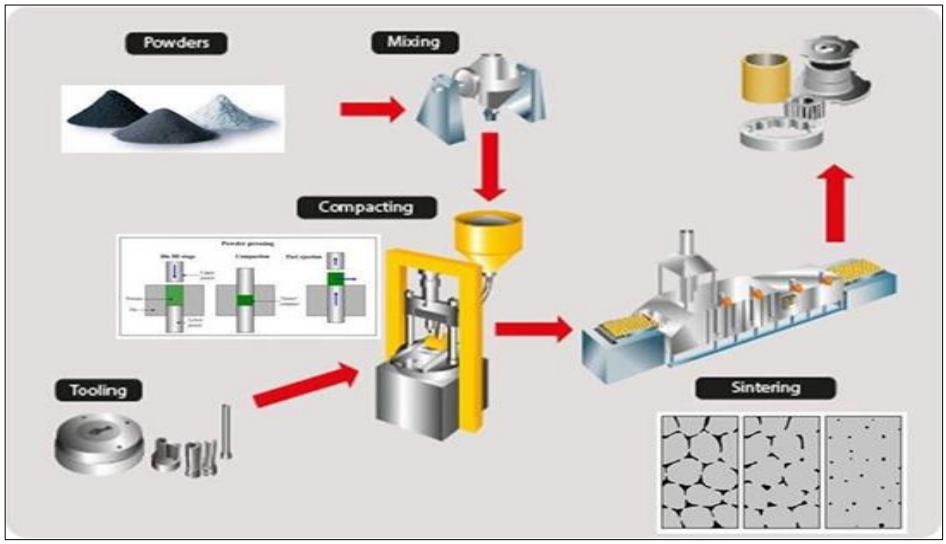

Figure 10. Powder metallurgy stages [31].

4.1. POWDER PRODUCTION METHODS

Practically, any metal can be transformed into a powder form. Normally, any of the three methods are used to produce metallic powders on a commercial scale. They require energy input for increasing a metal's surface area, and include atomization, chemical, and electrolytic methods. Figure 11 is given below to explain the powder production methods:

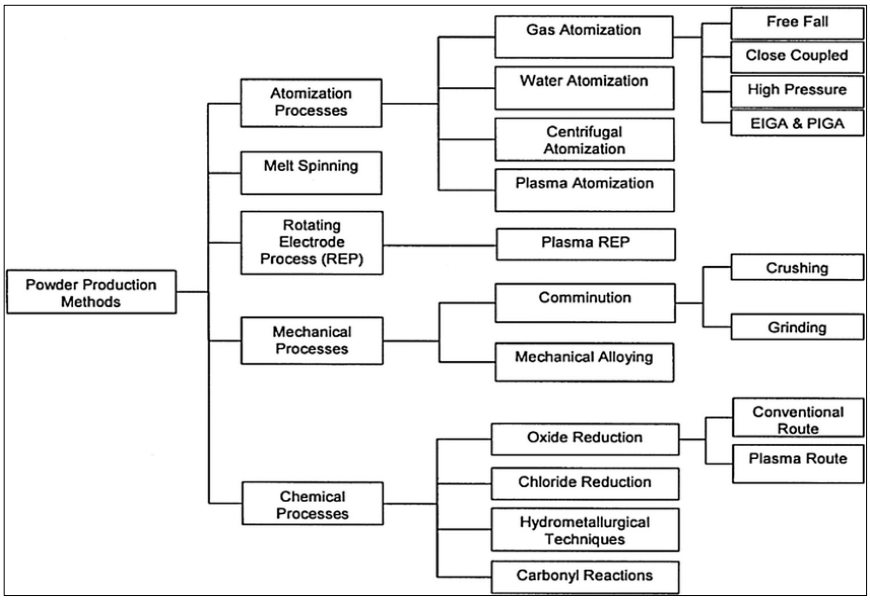

Figure 11. Powder Production Methods [31].

4.2. PRODUCED BY POWDER METALLURGY: PART CHARACTERIZATION IN MATERIALS

4.2.1. Powder Sampling

The grain size and shape of powdered metals play a significant role in processing and performance. Thus, understanding and knowledge of powder size and shape are necessary to improve and control different industrial processes. Because of large lot sizes, measuring an entire powder batch is impractical; therefore, a small representative sample is taken from the batch and characterized. Sampling must be judiciously done to ensure that the smaller samples' measured properties represent the entire powder batch. In another NIST report, a detailed synopsis of the powder

sampling techniques has been mentioned, which shows how the particle size and distribution of ceramic powders are determined [4]. It is preferable that the powder is in motion when a sample is taken from a batch of powder (it means that the powder is poured from one container to another). If the motion is impossible, a static sampling procedure can be initiated to take the sample using a device called “sample thief,” as shown in Figure 1. It is actually a rod that is equipped with a sampling chamber and a device that opens or closes the sampling chamber at the operator’s end [32].

4.2.2. Particle Size Measurement

For particle-size measurement, laser-based techniques have become important in many disciplines, including combustion research. Instruments were continuously developed to meet the demands, such as geometric accuracy and other needs of research and industrial applications.

4.3. COMPRESSION AND PRESSING OF POWDERS

The powder compaction procedure makes a compact metal powder with the help of a die applying high pressures. Conventionally, a punch tool is below the cavity when the tools are vertically oriented. Then, the powder is compacted to form a specific shape, after which it is ejected from the die cavity. In many such applications, the components require some additional work for the required usage that makes it a cost-effective manufacturing process. The compacted powder’s density increases when pressure is applied to it. The typical pressure range is 80-1000psi (0.5-7MPa), and it is possible to exert pressures from 1000 to 1,000,000psi. A 10-50t/in² (150-700MPa) is the generally applied pressure for metal powder compaction. Working with multiple lower punches is essential for maintaining the same compression ratio with more than a single height or level. A single-level tooling process makes a cylindrical work piece; however, the common multiple-level tooling produces a more complex shape. The standard production rate is 15-30 parts per minute [33].

4.3.1. Unidirectional Compression

Some direct or indirect compressive loads inherently exist in many structural systems. For an effective structural design, understanding the materials' or structures' behaviors under compressive loading is essential. It happens because compressive stresses, in most cases, control the failure mechanism. Bulking, which can occur locally or globally, is another process that occurs in conjunction with compression loading. In either scenario, it substantially reduces the structural effectiveness of the system and results in underutilization of the underlying material qualities, making the structure extremely vulnerable to flaws. In Fiber Reinforced Plastic (FRP) composites, the micro buckling of the fibers can cause the composite structures' compressive failure. In composite materials, this kind of failure is characterized as a material failure [34].

Direct compressive loading is efficient for various structural applications because bending or impact loading causes compressive stresses to develop in a structural part. Additionally, it is observed that typically, compressive strength is less compared to tensile strength, suggesting that compressive pressures may cause failure [34].

It is difficult to gauge and anticipate compressive strength. The theoretical work on the unidirectional (UD) composites' compressive behavior dates back to 1965. The UD composites' compressive strength has been predicted by Rosen [1]. Schultheisz, and Waas [3,4] and Camponeschi [2] have written thorough analyses of the composites' compression behavior. Recently, various compressive behavior prediction models for UD composites were created by some researchers. It hasn't been entirely settled yet. It occurs as a result of several factors having an independent or combined influence on behavior. In composites' manufacturing, defects are inherent, which affect how these materials behave when loaded. Because of the difficulties in forecasting the defect size and modeling, which led to some empiricism in some models, the defects are more prominent in compressive behavior. Because of the challenges in accurately estimating true compressive strength experimentally, another issue arises. The test fixture type, specimen geometry, load introduction technique, and fixture alignment during the testing and tabbing operations all exhibited high sensitivity to the results, In order to design using UD composites, a unified perspective of the data from many models and

the dependability of the testing techniques are crucial. The models were not compared because several prediction models were published in recent literature to assess the compressive behavior of UD composites. These models rely on the fibers being misaligned throughout manufacturing, and the misalignment level can vary between samples. The models of various researchers have been compared to various sets of experimental data. It is necessary to compare models to experimental results in order for them to be useful. It is possible for someone to have simple and computationally and easily usable analytical models for estimating compressive strength [38].

4.3.3. Cold Isotactic Compression

Since productivity and quality have been in focus for decades, manufacturers successfully used Cold Isotactic Pressing (CIP) worldwide. Moreover, CIP is applied for consolidating ceramic and metal powders to make a green part, which can be treated further, for example, machining, sintering, or rolling. At conventional pressures, that ranges within 1,035-4,138 bars (15,000-60,000 psi). The ambient temperature goes up to a maximum of 200°F (93°C), and the CIP achieves 95% ceramics' theoretical density, which is proven for high-performance components[35].

Cold Isotactic Pressing is commonly applied for compressing graphite, consolidation of ceramic powders, electrical insulators, fine ceramics for medical and dental applications, and refractories. Now, the technology has further expanded into new applications, for example, coatings of an engine's valve parts minimize cylinder heads' wear, sputtering targets pressing, telecommunications, electronics, automotive, and aerospace industries [35].

4.3.4. Hot Isotactic Compression

This manufacturing process reduces the metal porosity and increases the densities of several ceramics, and it improves the workability and other mechanical properties of a material. This procedure generates waste as well; for instance, radioactive waste (additives comprising waste) is typically contained in a canister with a thin metal wall. The adsorbed gases are expelled with high heat during the heat cycle, and the

remaining material is compressed with argon gas to reach its densest possible state. Because it can shrink steel canisters, this approach is utilized to minimize space in disposal containers and for transportation. Although it was created in the 1950s at the Battelle Memorial Institute, it has been utilized since the 1960s to manufacture nuclear fuel for submarines [40].

Inactive ceramics are also prepared with it. It has been approved by the Idaho National Laboratory to combine radioactive ceramic wastes. After producing molybdenum-99, ANTSO (Australia's Nuclear Science and Technology Organization) has been employing HIP as a method to immobilize radioactive waste [2]. The HIP method exposes components to increased temperatures and isotactic gas pressures. Argon is the most often utilized gas for pressurizing. Additionally, the material is protected from a chemical reaction using an inert gas. Choosing the right metal can reduce the detrimental impacts of chemical reactions. Normally, depending on the desired redox conditions, stainless or mild steel, nickel, or some other metal can be chosen. The pressure inside the vessel rises as the chamber gets warmer. Many systems employ coupled gas pumping to maintain the required pressure level. You can exert pressure on the object in all directions (isotactic pressure).

This technique can convert metal powders into compact solids for casting processing. The inert gas pressure range is 7,350-45,000 psi (50.7-310 MPa) with 15,000 psi (or 100 MPa) the most typical. Aluminum casting soak temperature range is 900-2400°F (482 -1320 °C) for the majority of nickel-based super alloys. Pressure and heat are applied simultaneously after HIP treatment for castings because it eliminates micro porosity and internal voids by diffusion bonding, creep, and plastic deformation, increasing the component's fatigue resistance. The main uses include micro shrinkage reduction, powder metals' consolidation, and metal cladding reduction of ceramic composites. In order to fabricate metal matrix composites, which is frequently done as a post-processing step in additive manufacturing, hot isotactic pressing is a part of the sintering process (powder metallurgy) as showed in Fig 12 [40].

Figure 12. Hot Isostatic Compression [35].

4.4. SINTERING OF POWDERS

To impart strength and integrity, sintering is a heat treatment applied to a compact powder. The sintering temperature is normally below the metal's melting point, which is a significant property of Powder Metallurgy as explained in Fig 13.

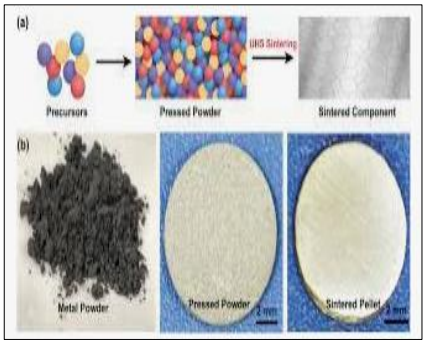

Figure 13. Sintering of Powders[35].

4.5. ANALYSIS OF MATERIALS PRODUCED BY POWDER METALLURGY METHOD

A significant benefit of the powder metallurgy process is its design flexibility with dimensional accuracy and superior properties, so the PM process is now becoming more feasible and profitable for various metal forming processes. Its production cost is lower when the number of PM components, which have a higher than economic quantity, are produced. PM is an attractive option because of its capability to produce different parts with different dimensions, for example, precise (close tolerance), high-performance, and porous components in a cost-effective way. The PM parts of stainless steel show a growing and important segment of powder metallurgy. Stainless

steel powders have been selected to replace PM ferrous alloys because of their superior characteristics. Their characteristics include oxidation resistance, corrosion resistance, mechanical properties (impact strength and ductility), and wear resistance. In several applications, including agriculture, aerospace, automotive, appliances, chemical, building and construction, hardware, electrical and electronic, jewelry, industrial, medical, marine, recreation and leisure, and office equipment, stainless steel Series 300 powders are extensively used. In PM applications, stainless steel Series 400 powders are commonly used. It is mainly because of their fairly good corrosion resistance, ferromagnetic properties, low cost, and good strength. Series 400 alloys are found in automotive parts. Their examples include an antilock brake system (ABS), automotive rearview mirror mounts, and sensor rings. Many components of the exhaust systems include hot exhaust gas oxygen sensors (HEGOS) and coupling flanges. In recent times, the interest of the researchers has diverted to the potential for 400 series PM parts, specifically in the mentioned automotive exhaust system components [42].

PART 5

EXPERIMENTAL METHOD

5.1. INTRODUCTION

In this study the powder metallurgy (PM) will be applied to produce the desired compositions of Nb-V PM alloy steel then the impact of various Ni and micro-alloying element concentrations on the mechanical characteristics and microstructure will be investigated, in addition wear behaviors will be investigated as well.

5.2. PRODUCTION PROCEDURE OF PM STEELS

The current study PM steel samples containing, Graphite, iron, vanadium niobium, and nickel powder were utilized to create the steel specimens. Niobium vanadium, graphite, iron, and nickel powders purities and sizes explained in the table 2.

Table 2. powders purities and sizes[36].

Id. No	Elemental powder	Powder diameter (μm)	Purity (%)
1	Niobium	45	99.8
2	vanadium	44	99.5
3	graphite	20	96.5
4	iron	180	99.9
5	nickel	5	99.7

The powders were weighed using RADWAG AS-60-220 C/2 using a 104 g precision scale before the mixing operation began as shown in the Figure 14.

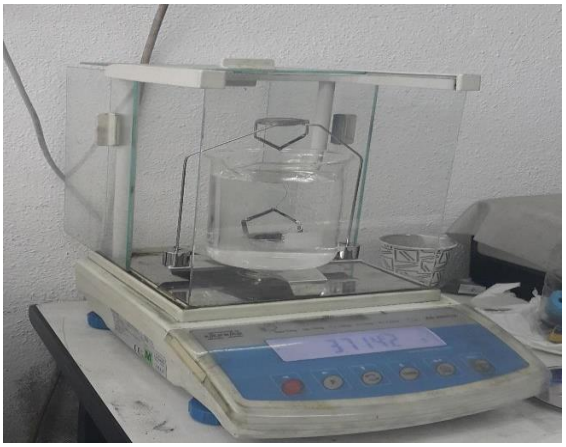

Figure 14. RADWAG AS-60-220 C/2.

The powders' chemical makeup has been displayed in Table 3. Using TURBULA T2F device with 3D motion as shown in Figure 15, Fe-C-NbV-xNi particle-mixing was continued for an hour. The powders were pressed with a 100-ton by the hydraulic press (Hidroliksan, Konya, Turkey) while applying 750MPa pressing pressure.

After pressing was finished, sintering was started in an environment of argon at 1400°C for two hours. The sintering process is carried out in an atmosphere-controlled tube furnace which is shown in Figure 16. The specimen densities were determined with the help of Radwag density kit (manufactured by Bruker Alpha, Bursa, Turkey) and ASTM B 328-96. Table 3 shows a list of the alloys' chemical make-ups and densities.

Table 3. Chemical compositions of powder metal steels[36].

Compound	Graphite (wt%)	Nb (wt%)	V (wt%)	Ni (wt%)	Fe (wt%)	Densities (g/cm^3)
Fe+0.25C (Alloy-1)	0.55	-	-	-	rest	7.2837
Fe+0.25C+0.15(Nb+V) (Alloy-2)	0.55	0.075	0.075	-	rest	7.2787
Fe+0.25C+0.15(Nb+V)+5Ni (Alloy-3)	0.55	0.075	0.075	5	rest	7.4102
Fe+0.25C+0.15(Nb+V)+10Ni (Alloy-4)	0.55	0.075	0.075	10	rest	7.2347
Fe+0.25C+0.15(Nb+V)+13Ni (Alloy-5)	0.55	0.075	0.075	13	rest	7.5947
Fe+0.25C+0.15(Nb+V)+15Ni (Alloy-6)	0.55	0.075	0.075	15	rest	7.6724
Fe+0.25C+0.15(Nb+V)+20Ni (Alloy-7)	0.55	0.075	0.075	20	rest	7.5484
Fe+0.25C+0.15(Nb+V)+30Ni (Alloy-8)	0.55	0.075	0.075	30	Rest	7.2903
Fe+0.25C+0.15(Nb+V)+40Ni (Alloy-9)	0.55	0.075	0.075	40	rest	7.2231

Figure 15. TURBULA T2F device with 3D motion.

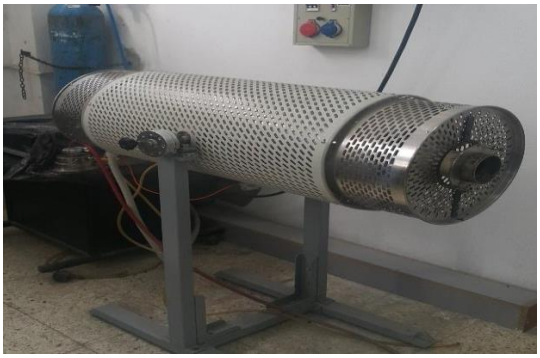

Figure 16. Atmosphere-controll duct furnace.

Moreover, under $HV_{0.5}$ load, the hardness tests of these parts were assessed using a hardness measuring device.

Nikon ECLIPSE L150 microscope (Melville, NY, USA) was used to conduct optical microscopy studies. The alloys' grain sizes were determined through a mean linear intercept method [12,13]. We used Rigaku Ultima IV diffract meters and Zeiss microscope for XRD and SEM, respectively, to conduct the microstructural and fracture surface examinations.

5.3 Corrosion measurement procedure

Electrochemical potential dynamic tests are applied to determine the corrosion performances of the alloys in 3.5% NaCl solution. A "Parstat 4000 (Rotalab, Ankara, Turkey)" was applied as a potentiostat as shown in Figure17, with an electrochemical cell in which a saturated calomel electrode (SCE) was used as a reference electrode. Later 3 h of immersion of the samples, potentials were applied between −0.5 and 0.5 V versus open circuit (O.C.) potentials with a scan rate of 2.5 mV /s. Here, anodic and cathodic regions were scanned separately (the O.C. potential was selected as the first scanning point, so O.C. potentials are equal to corrosion potentials) in demand to maintain more reliable surfaces of the working electrodes through the measurements of corrosion currents and stabilize the effects of applied potentials. In our setup, we tried our best to place vessel lugging as close to working electrode as possible. This setup should reduce any extra voltage drop. Before the measurements the surfaces of the samples were prepared with a series of different meshes of abrasive papers (400,

600, 800, 1000, 1200 and 2000 meshes, coarse to fine). Then all of them were cleaned by ethyl alcohol and distilled water.

Figure 17 . Parstat 4000 (Rotalab, Ankara, Turkey.

The above device has been used to achieve a potentiodynamic corrosion investigation using the parametersexplained in Table 4, at the room temperature 25 ºC.

Table 4. Potentiodynamic corrosion test parameters.

Corrosion test	Potentiodynac
Scan rate	2.5 mV/s
Reference electrode	a saturated calomel electrode (SCE)

5.4 Wear measurement procedure

In this study, powder metallurgy is used to produce steel samples with the required compositions. In the study, we examined the effects of different Ni concentrations and micro-alloying components on the mechanical properties and microstructure. Powders of iron, graphite, niobium, vanadium, and nickel were used to create the steel specimens.

For SEM, a Zeiss microscope was used for microstructural and fracture surface examinations, respectively. The micro harnesses of these parts were determined using a SHIMADZU hardness test device (MCT-W, Shimadzu, Tokyo, Japan) [37].

Surface grinding was done using 800 mesh grinding paper, and PM samples were subjected to reciprocating wear tests utilizing a UTS-10 tribometer tester. For the wear test, a steel ball made of AISI 52100 was used, and a 10 mm stroke distance was maintained. There are a total of 1000 meters. The applied loads are 15 and 30 N, and the shear speed is 72 mm per second. The material was cleaned with ethanol following each abrasion test, and wear weight loss was determined using an electro balance with a precision of 0.1 mg. using the device's software, the depth of wear, friction coefficient, and friction force were computed [37].

For the experiments, a ball-on-plate wear instrument was utilized. A wearable device and a wear cell are shown in Figure 18. The size of the wear sample was 1 x 2 cm. AISI 52100 (100Cr6) steel ball is used as an abrasive ball. After each test, the steel ball's deformed surface was swapped out, and each test was carried out under identical circumstances. A 50-rpm sliding speed was maintained. A 10 mm stroke was used during the wear test, which was conducted at a distance of 1000 m [37].

Dry and corrosive media were the two categories from which the wear media were chosen. Dry the paste in an open area while it's still warm. The corrosive wear medium was a 3.5% NaCl solution in clean water. 100 ml of solution were used for each test. The fluid introduced to the wear cell in corrosive wear was changed at the conclusion of each test.

At the conclusion of each experiment, the material's weight loss was calculated with an accuracy of 0.0001 gr. After the wear test, SEM photographs and EDS analysis of the wear surfaces were gathered. After analyzing abrasion traces with a surface profilometer instrument, the wear depth and abrasion cross-sectional area were estimated. The wear surfaces of specimens made of PM steel were then examined using SEM (Figure 18) [37].

Abrasion tests have not been performed for Alloy 9 that is because after hardness and corrosion analysis, no abrasion test was required for steel containing 40% Ni.

Figure 18. Wear unit.

PART 6

RESULTS AND DISCUSSION

6.1 EVALUATION OF CORROSION TEST

The Tafel curves in figure19, and the Ecorr and Icorr values in table 5, obtained from the potentiodynamic corrosion tests and corrosion rates were calculated using the relevant formulae given in ASTM-G102 [38].

Alloy equivalent weight can be calculated by the Equation below,

$$\mathrm{EW} = \frac{1}{\sum \frac{\mathrm{nifi}}{\mathrm{Wi}}} \tag{6.1}$$

Where EW is an equivalent weight ,ni the valence of the ith element of the alloy, and fi the mass fraction of the ith element in the alloy and Wi: the atomic weight of the ith element in the alloy [38].

In addition, Corrosion rate (CR) of samples can be calculated by Faraday's equation,

$$\mathrm{CR} = \frac{\lambda * \mathrm{icorr}}{\mathrm{d}} * \mathrm{EW} \tag{6.2}$$

Where $\lambda = 3.27 \times 10\text{-}3$ (mm. g)/ (mA. cm. year), and d is density in g/cm^3 [38].

It is clear that Tafel description of overall corrosion dynamics must be possible. It seems that addition of Nb and V into pure steel leads to a significant increase of corrosion resistance [39] .

There are many studies in the literature that explained that microalloyed steels have good corrosion resistance compared to unalloyed steels. Uygur et al, examined the corrosion properties of unalloyed steel and microalloyed steel with different ratios of Nb–V microalloying elements by powder metallurgy [40].

From the results that have been obtained it is clear that the corrosion resistance increases almost three times with the addition of 0.075 Nb and V by weight of unalloyed steel. The results obtained are similar to those in this study. The grain size has decreased as a result of the addition of Nb–V to unalloyed steels.

It is informed us that the fine pearlite ferrite structure is more resistant to corrosion than the coarse pearlite ferrite structure. When the grain size refinement's that will effects on corrosion resistance were investigated in the literature and similar conclusions were reached. Ura-Bin´czyk et al. [41] informed us that grain refinement causes a more intense and uniform passive film on the N80-1 steel surface. Thus, it has been observed that N80-1 steel is more corrosion resistant than K55 steel.

Table 5. Ecorr and Icorr alloy values.

Alloy	Specimen	Ecorr (V)	Icorr (μA/cm2)	CR (mm/year)
A-1	Pure Steel	−0.68	37.9	0.48
A-2	(V + Nb) Steel	−0.66	12.5	0.16
A-3	(V + Nb) Steel + 5% Ni	−0.58	14.9	0.19
A-4	V + Nb) Steel + 10% Ni	−0.54	23.8	0.30
A-5	(V + Nb) Steel + 13% Ni	−0.49	23.9	0.30
A-6	(V + Nb) Steel + 15% Ni	−0.52	18.3	0.23
A-7	(V + Nb) Steel + 20% Ni	−0.54	9.3	0.12
A-8	(V + Nb) Steel + 30% Ni	−0.45	6.12	0.08
A-9	(V + Nb) Steel + 40% Ni	−0.40	2.3	0.03

The addition of Nickel to the microalloyed steel, leads to a quite complex behavior. It is clear that from the Figure 19, lower corrosion resistance with increasing Ni content for alloys with concentrations lower than 10 wt. % Ni. However, this behavior radically reversed for alloys with Ni concentrations higher than 13 wt. % Ni. Further

addition of Ni into NbV microalloyed steel that lead to converts these alloys to high corrosion resistant metallic systems, this dramatically coverts shown in the table 6 as well.

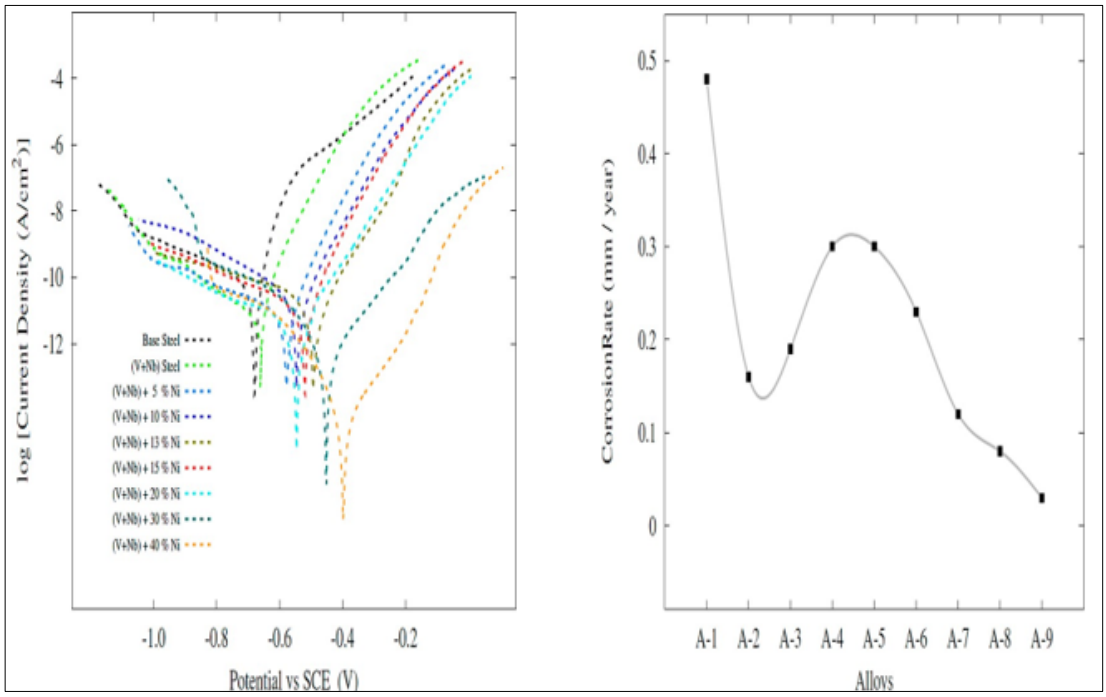

(a) (b)

Figure 19. Tafel curves (a) and corrosion rate curves (b) the alloys.

We noted that the best value of corrosion resistance is seen in steel containing 40% nickel by weight as shown in the fig 19 and the lowest value for Corrosion rate (CR) was in alloy 9 with (V + Nb) Steel + 40% Ni. In the literature, there are many studies are supporting our results[42]. Alharthi et al. has investigated the effect of the amount of nickel on the corrosion resistance of Fe-36% Ni and Fe-45% Ni alloys in 1M hydrochloric acid pickling solution. The EIS results showed that the polarization and surface resistances for the alloy with high Ni content were much higher. The results showed that the Fe-45% Ni alloy has much better corrosion resistance than the Fe-36% Ni alloy [43].

SEM images of the samples with Ni and without Ni after corrosion test are given in Figures 20 and 21. Whereas the samples without Ni have corrosion scales on the surface, it was observed that pittings localized on the alloy 3-NbV-5Ni after corrosion.

Figures 22 and 23 shows SEM image and mapping analysis of alloy 2-NbV-0Ni and alloy 9-NbV-40Ni respectively.

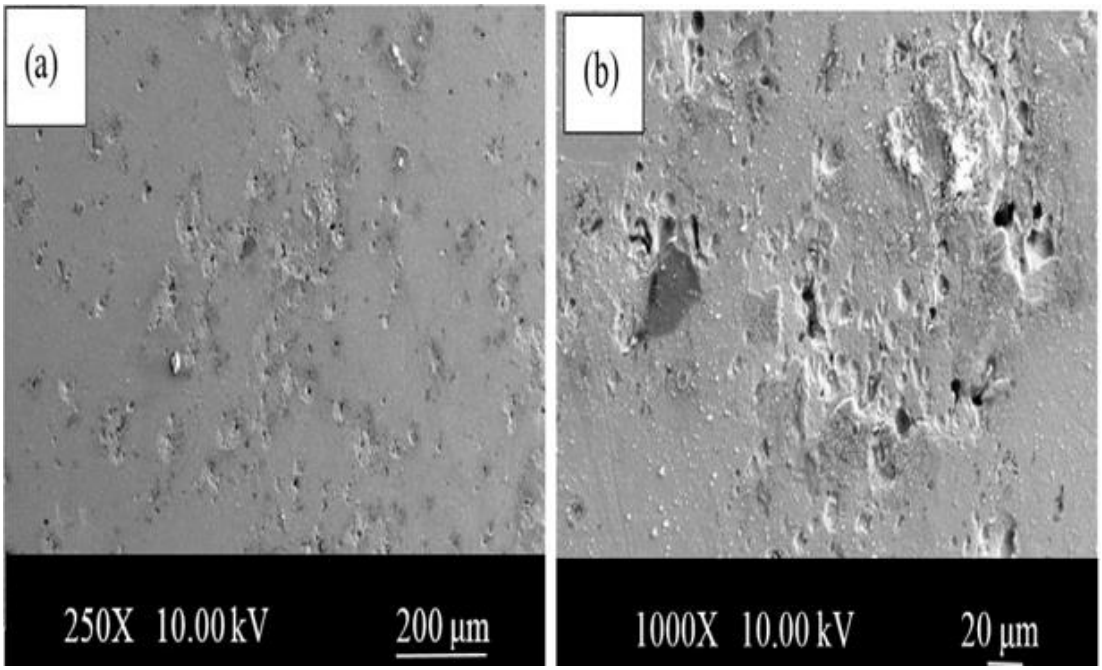

Figure 20. SEM images of the alloy 2-NbV-0Ni after corrosion (**a**) low and **b**) high magnification.

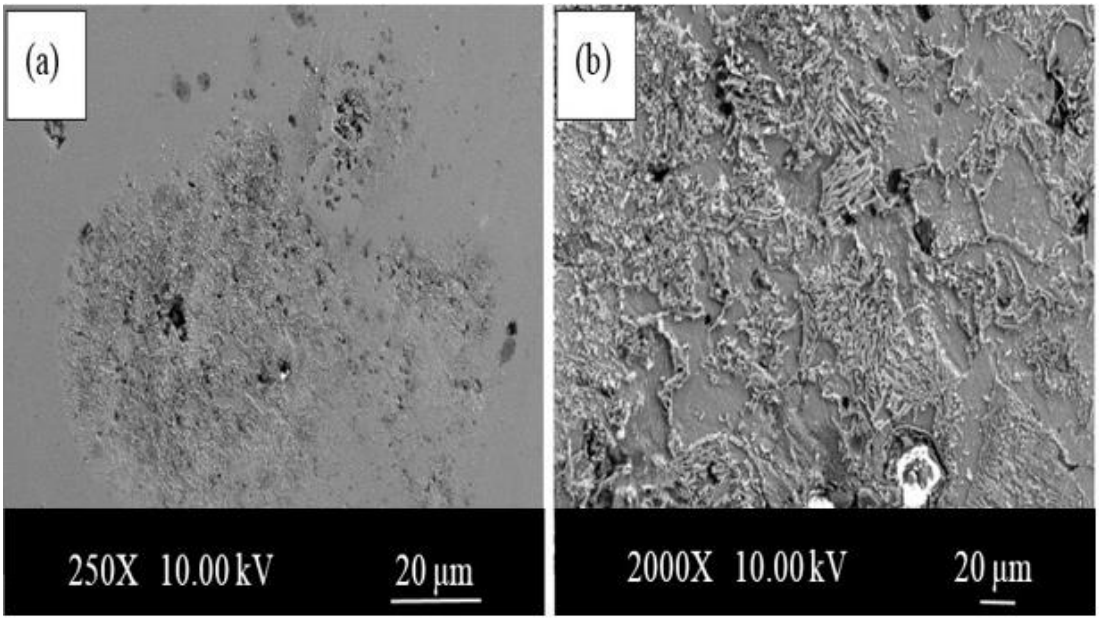

Figure 21. SEM images of the alloy 3-NbV-5Ni after corrosion (**a**) low and (**b**) high magnification.

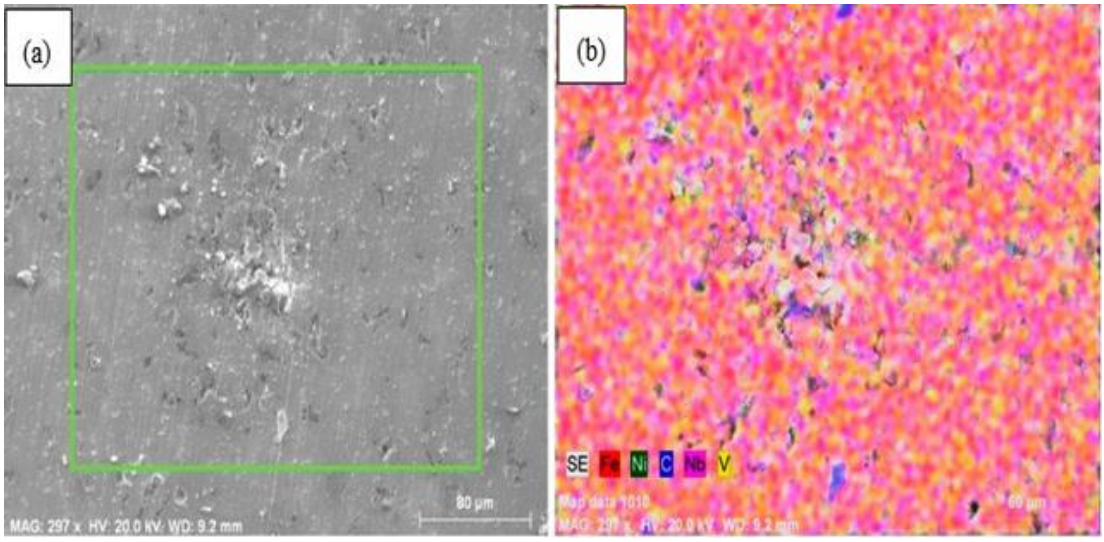

Figure 22. (a) SEM image and (b) mapping analysis of the alloy 2-NbV-0Ni after corrosion.

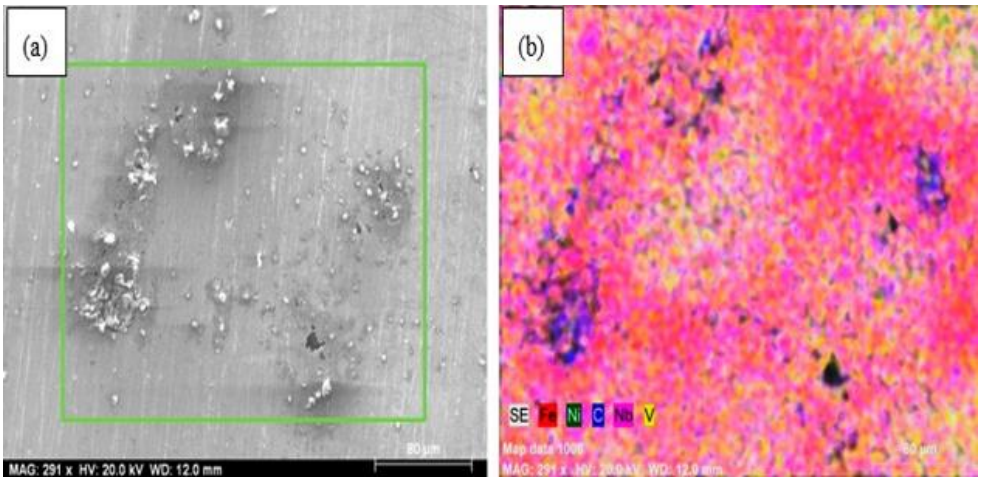

Figure 23. a) SEM image and (b) mapping analysis of the alloy 9-NbV-40Ni after corrosion.

6.2. WEAR RESULTS AND EVALUATION

The results of the wear test and hardness measurements of the samples prepared by mixing Nb-V with TM unalloyed steel are shown in Table 6 and Figure 24. The data gathered from the wear tests performed on the TM steel samples showed that the wear depth increased with increasing load. Because of the inclusion of microalloying components, Alloy 2 demonstrates a noticeably improved wear and hardness resistance despite having the same amount of carbon as Alloy 1. The precipitation of

microalloying elements and the narrowing of grain size are the key contributors to the enhanced mechanical properties.

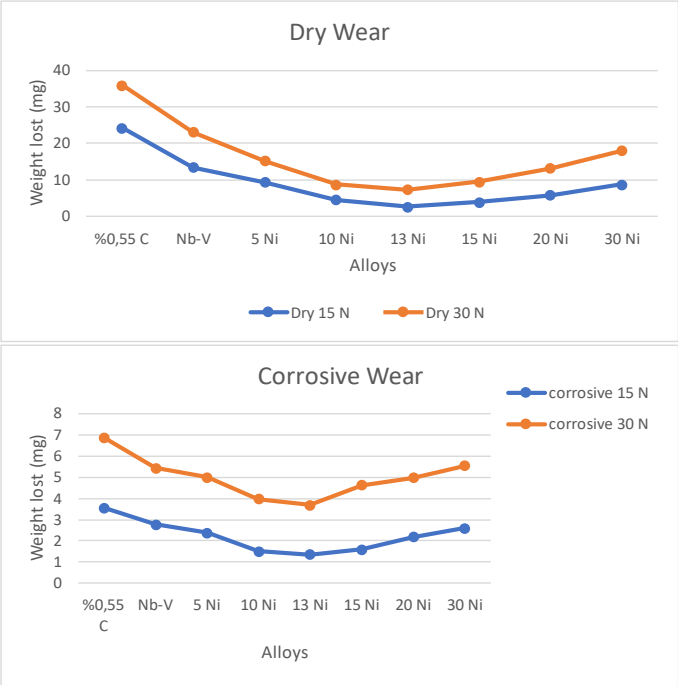

Figure 24. Weight loss graphs.

Table 6. Weight losses in milligrams results of TM steels sintered at 1400 °C.

Alloy	Specimen	Dry 15N(mg)	Dry 30N (mg)	Corrosive 15N(mg)	Corrosive 30N(mg)	Harness 0,5Hv[x][45]
A-1	Pure Steel	24.255	35,866	3,568	6,882	75
A-2	(V + Nb) Steel	13.466	23,118	2,776	5,450	125
A-3	(V + Nb) Steel + 5% Ni	9.430	15,187	2,388	5,008	160
A-4	V + Nb) Steel + 10% Ni	4,558	8,813	1,504	3,972	243
A-5	(V + Nb) Steel + 13% Ni	2,734	7,367	1,344	3,704	244
A-6	(V + Nb) Steel + 15% Ni	3,912	9,550	1,596	4,628	191
A-7	(V + Nb) Steel + 20% Ni	5,908	13,182	2,188	4,976	133
A-8	(V + Nb) Steel + 30% Ni	8,804	17,999	2,608	5,561	93

Niobium and vanadium microalloying elements precipitate as carbide, nitride, and carbonitrides during sintering and cooling. These compounds enhance the mechanical characteristics of micro alloy steels by processes like grain reduction, solid melt hardening, and precipitation hardening [44].

Due at, increased the low carbon steel's wear resistance and hardness by producing TiC-VC precipitates. Other research claim that the carbides and nitrides found in micro alloy steels increase the steel's hardness and tensile strength. According to the same research, solid melt hardening proceeds at a slow rate because of carbide and nitride precipitation [46].

After the TM samples were sintered at 1400 °C in an argon environment under 30N pressures for the wear test, the worn surface images were separately captured on the X250 and X500. The abrasive ball often creates lines parallel to the sliding direction when the images are examined. These lines show how the abrasive wear mechanism in steel produced by the TM process works (Figure 25).

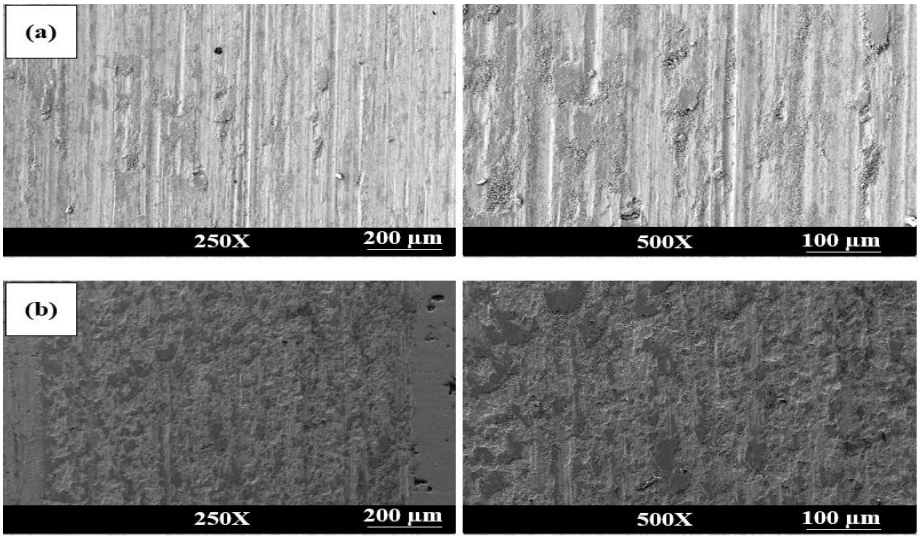

Figure 25. SEM images of the wear surface a)Alloy 1; b)Alloy 2 (250x-500x).

According to the SEM images taken from the wear surfaces, all materials have wear channels. It was also discovered that the scratches on the worn surface of unalloyed steel were deeper and thicker, but the scratches produced in the Nb-V added sample evolved in a shallower and thin shape. This is in line with the hardness values.

Erden et al. [47] added 0.1-0.15-0.2% by weight of Nb-Al powder to the matrix to study the friction-wear performance of the alloying element in NB-Al micro alloy steel. Unalloyed steel exhibited the lowest wear resistance, whereas alloys with 2% Nb-Al added had the greatest results.

It was also discovered that the alloys' hardness levels rose when the Nb-Al ratio rose. Similar conclusions were drawn from their examination of the wear surfaces, where they found that all materials shared the same wear mechanisms and that the presence of additional Nb-Al in the friction materials made the wear lines appear more shallow and thin. The addition of the Nb-V alloying element consequently increased the wear and hardness resistances. This is caused by strength-enhancing processes, such as aggregation hardening, precipitation hardening, and grain size reduction induced by the precipitates such as VC(N), NbVC (N), NbC(N).

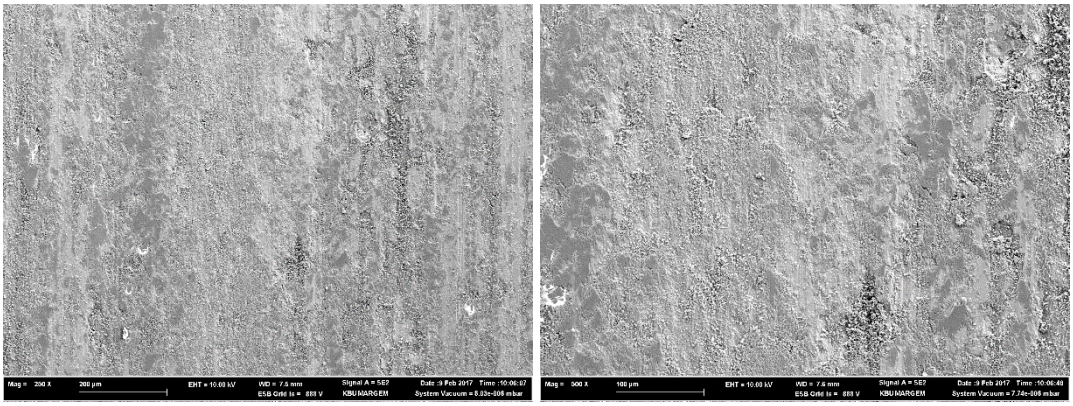

5Ni

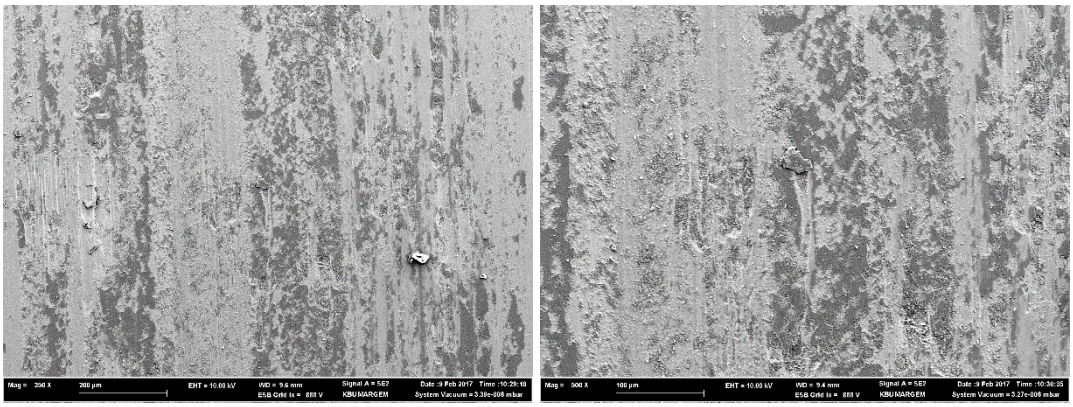

10Ni

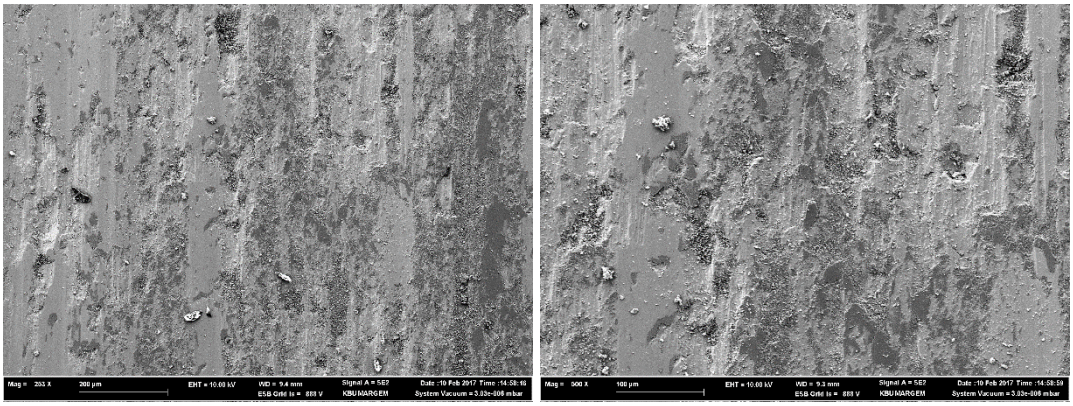

13Ni

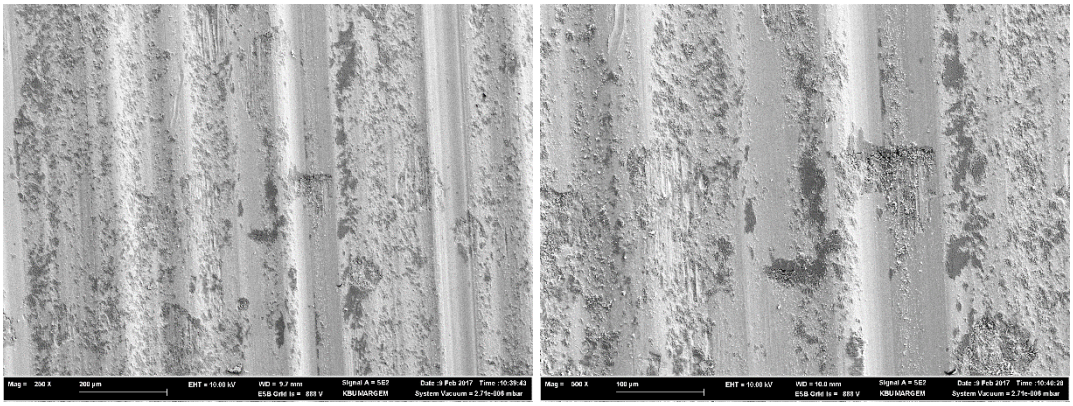

15Ni

Figure 26. Dry surface SEM images.

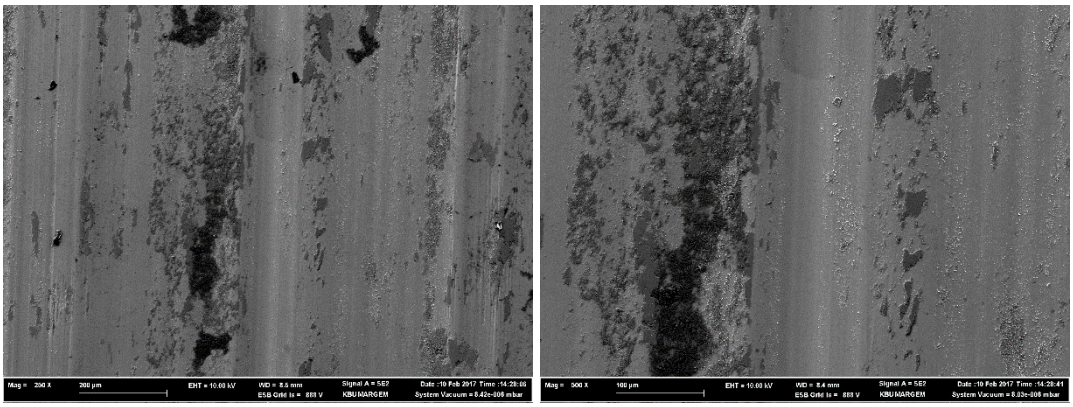

16Ni

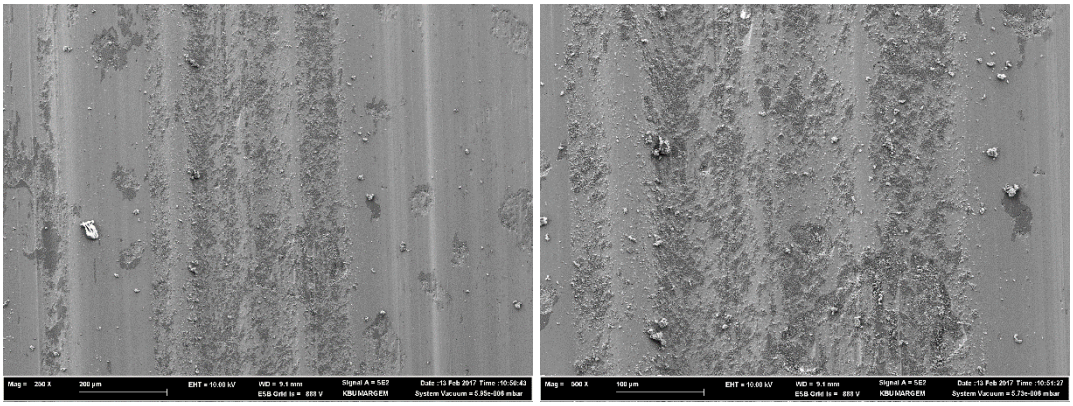

20Ni

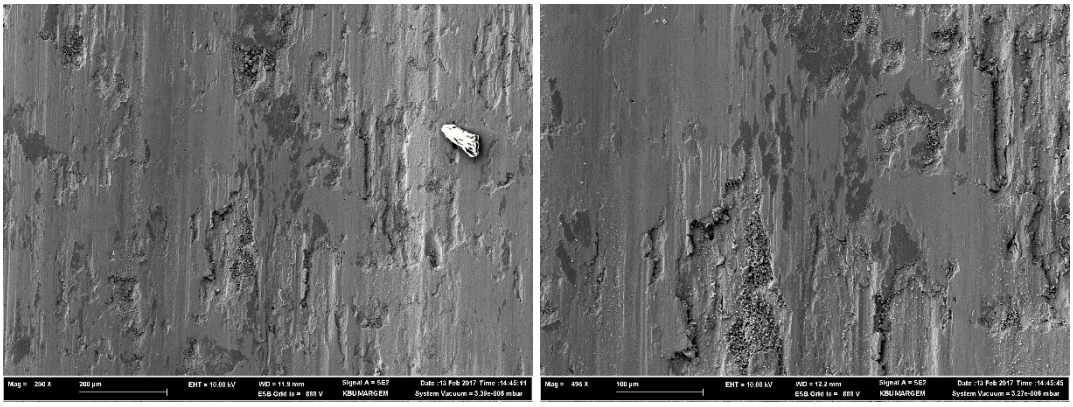

30Ni

Figure 27. (continues).

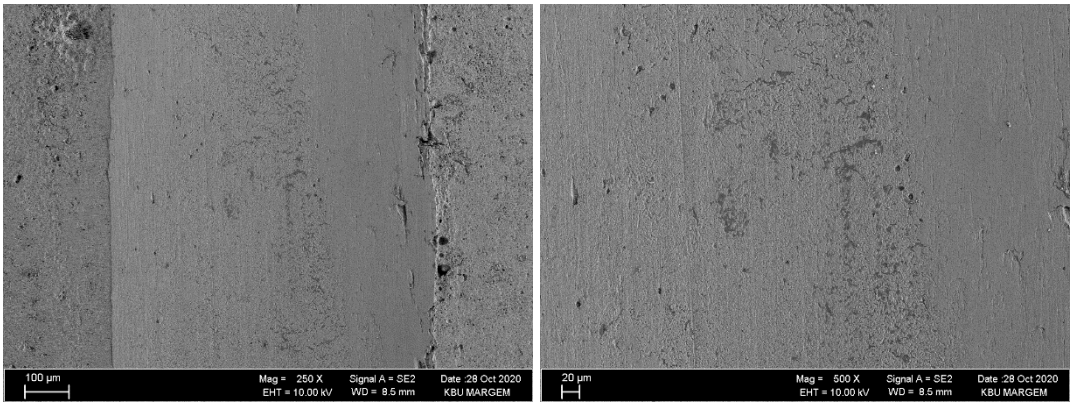

Fe-C corrosive wear surface

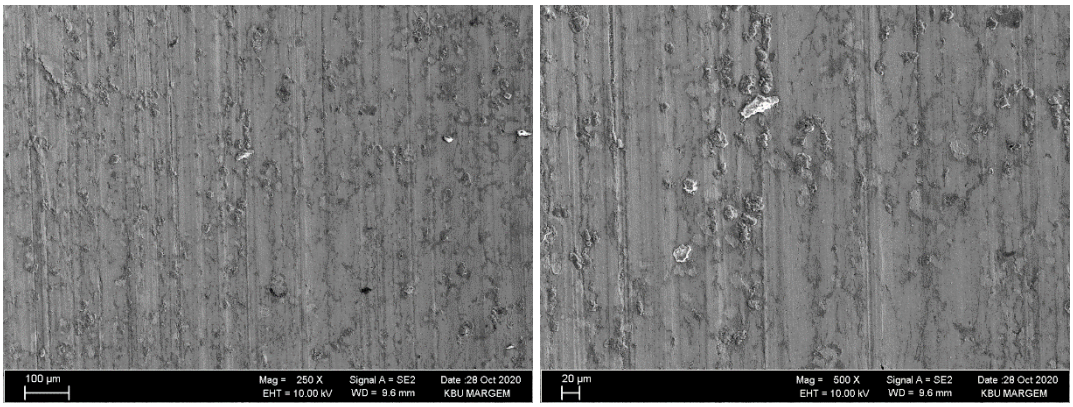

Fe-C-NbV corrosive wear surface

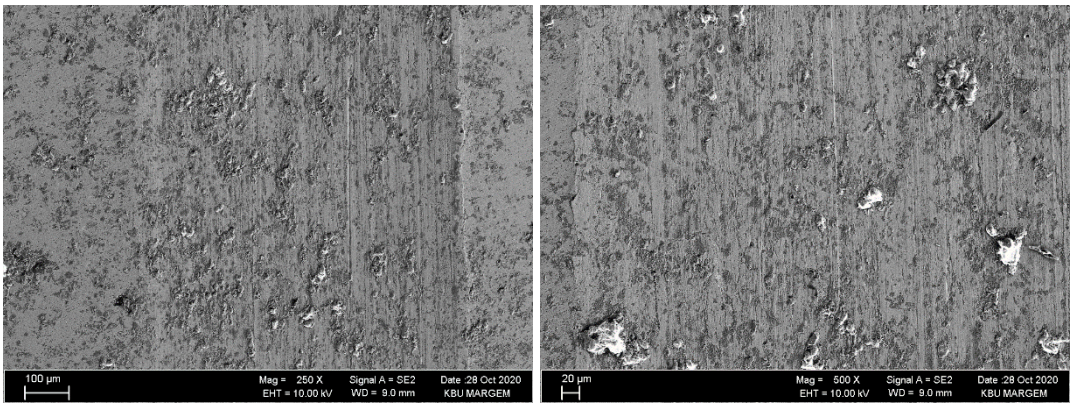

Fe-C-NbV-5Ni corrosive wear surface

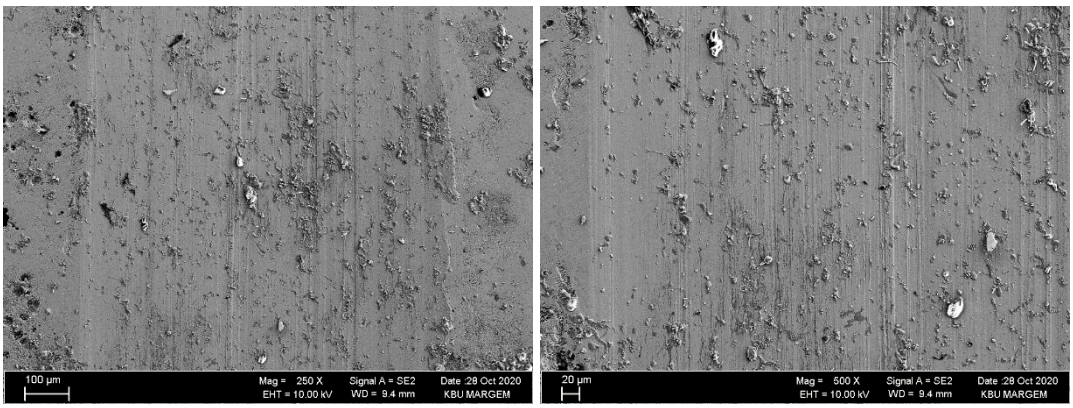

Fe-C-NbV-10Ni corrosive wear surface

Figure 28. Corrosive Wear surface SEM images.

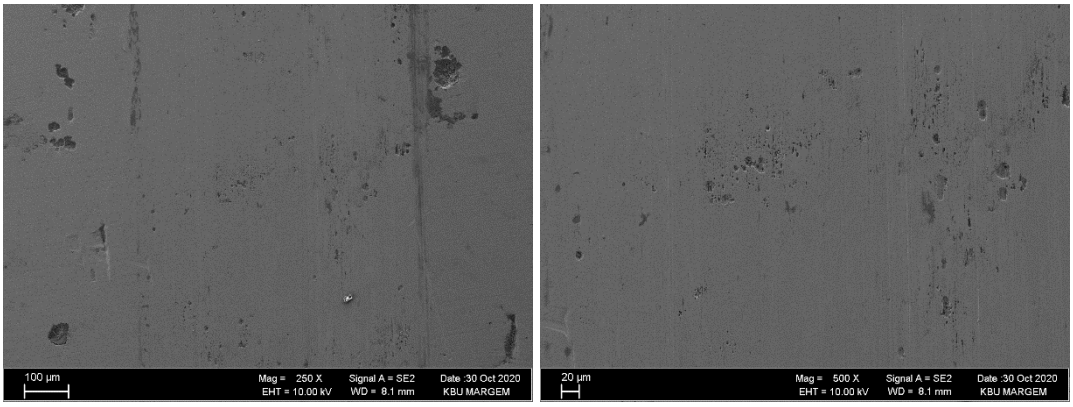

Fe-C-NbV-13Ni corrosive wear surface

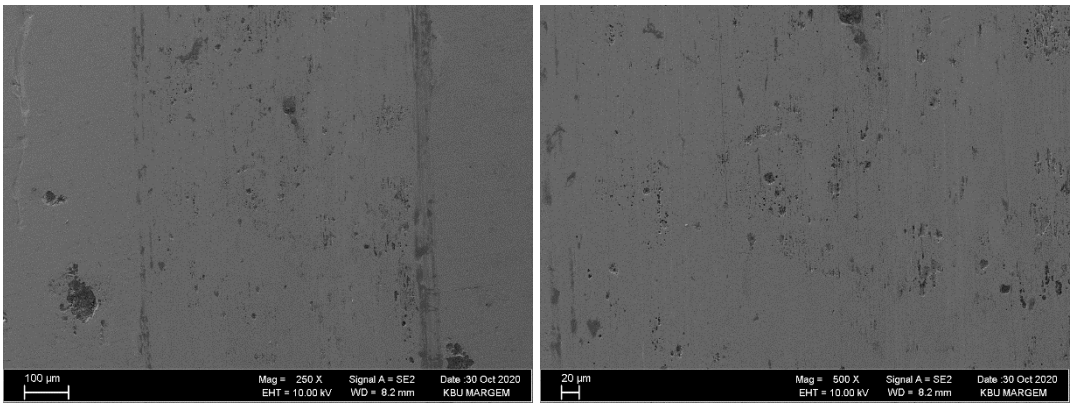

Fe-C-NbV-15Ni corrosive wear surface

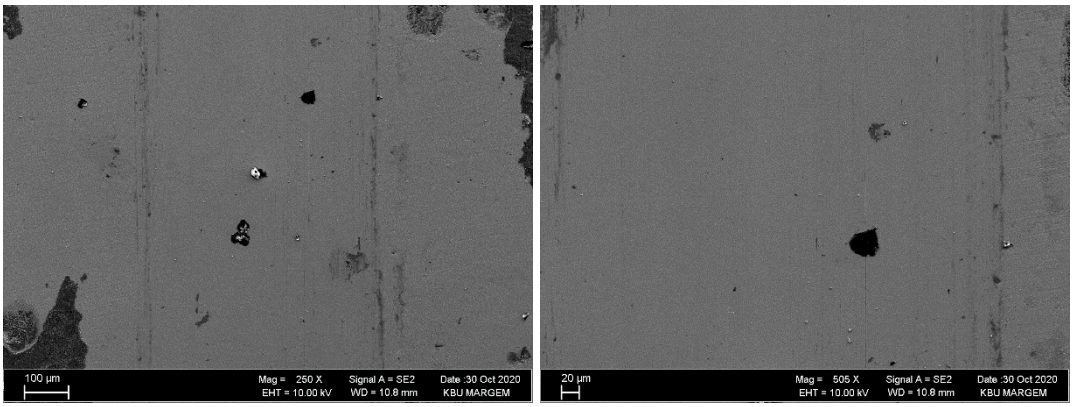

Fe-C-NbV-15Ni corrosive wear surface

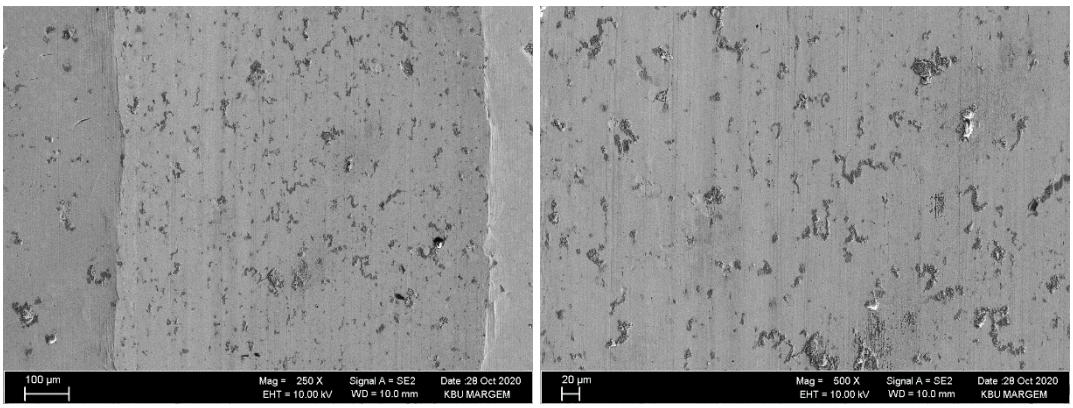

Fe-C-NbV-20Ni corrosive wear surface

Figure 297. (continues).

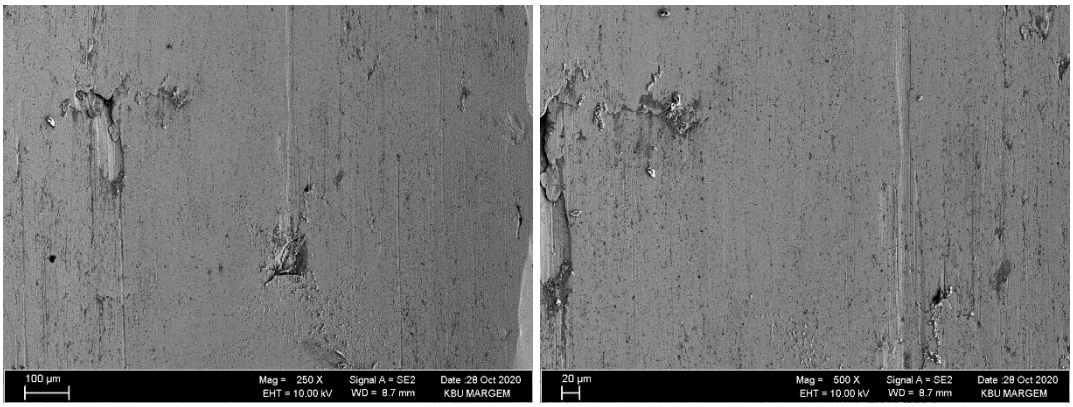

Fe-C-NbV-30Ni corrosive wear surface

Figure 307. (continues).

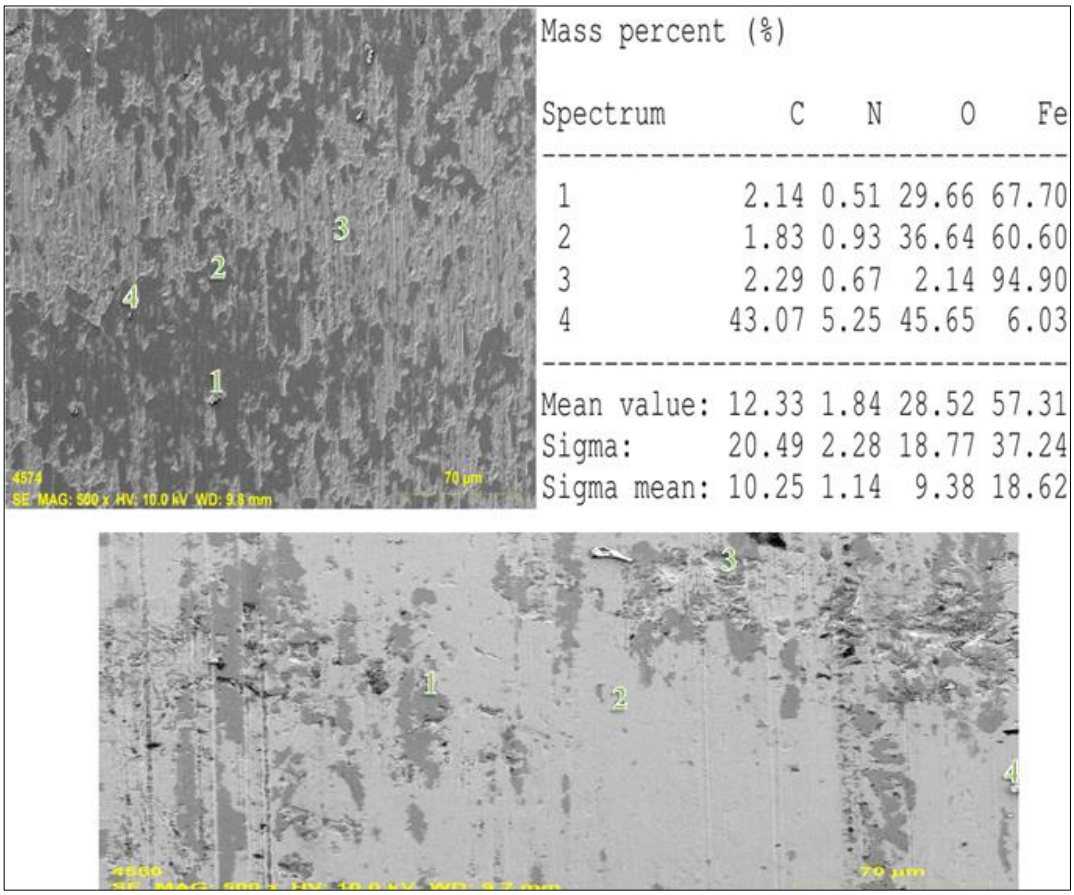

Figure 31. SEM EDS results from wear surface.

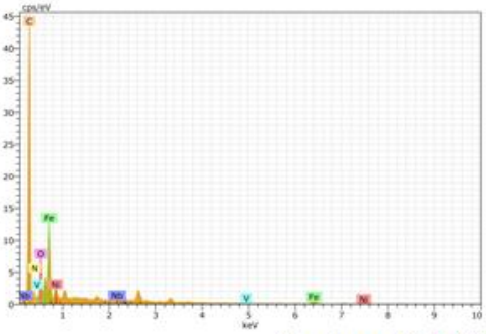

Mass percent (%)

Spectrum	C	N	O	V	Fe	Ni	Nb
1	3.00	0.43	32.09	0.00	63.75	0.72	0.00
2	3.67	0.62	0.99	0.00	86.24	8.48	0.00
3	8.78	0.73	3.41	0.02	82.67	4.39	0.00
4	57.16	9.22	15.58	0.38	13.42	3.98	0.26
Mean value:	18.15	2.75	13.02	0.10	61.52	4.39	0.07
Sigma:	26.13	4.32	14.23	0.19	33.55	3.18	0.13
Sigma mean:	13.07	2.16	7.11	0.09	16.78	1.59	0.07

Spectrum NbVCN Dry Precipitate

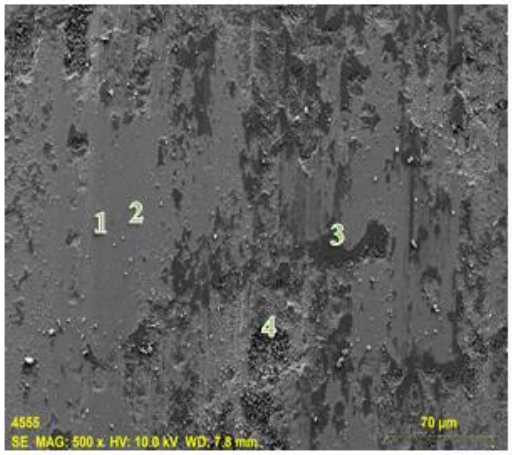

Mass percent (%)

Spectrum	C	N	O	V	Fe	Ni	Nb
1	3.04	0.61	2.13	0.12	81.44	12.52	0.14
2	3.53	0.53	0.77	0.07	82.65	12.34	0.11
3	2.20	0.54	33.27	0.04	61.20	2.63	0.12
4	3.54	0.70	6.90	0.05	80.64	8.07	0.10
5	1.43	0.29	22.35	0.00	74.10	1.83	0.00
Mean value:	2.75	0.53	13.08	0.06	76.00	7.48	0.09
Sigma:	0.92	0.15	14.17	0.04	8.92	5.12	0.05
Sigma mean:	0.41	0.07	6.34	0.02	3.99	2.29	0.02

13Ni Dry

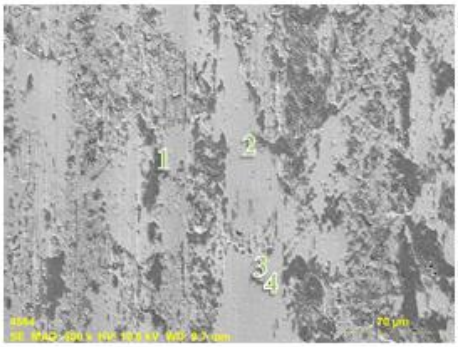

Mass percent (%)

Spectrum	C	N	O	V	Fe	Ni	Nb
1	2.42	0.33	34.81	0.00	61.97	0.47	0.00
2	2.69	0.67	1.35	0.01	79.75	15.52	0.00
3	2.90	0.78	2.82	0.14	84.28	9.01	0.07
4	2.55	0.56	1.19	0.26	79.11	16.32	0.00
Mean value:	2.64	0.59	10.04	0.11	76.28	10.33	0.02
Sigma:	0.21	0.19	16.53	0.12	9.81	7.34	0.04
Sigma mean:	0.10	0.10	8.26	0.06	4.91	3.67	0.02

15Ni Dry

Figure 328. (continues).

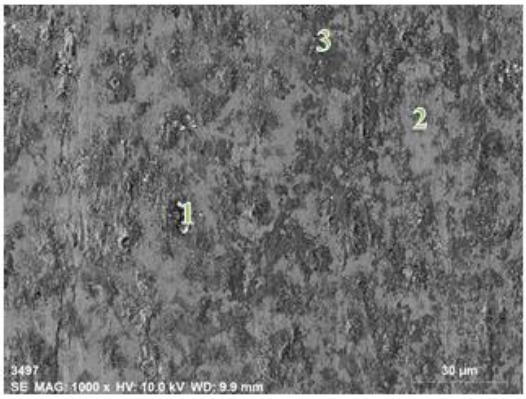

Mass percent (%)

Spectrum	C	O	Fe
1	11.27	52.19	36.54
2	12.98	13.61	73.41
3	10.96	45.99	43.05
Mean value:	11.74	37.26	51.00
Sigma:	1.09	20.72	19.68
Sigma mean:	0.63	11.96	11.36

Corrosive Fe-C

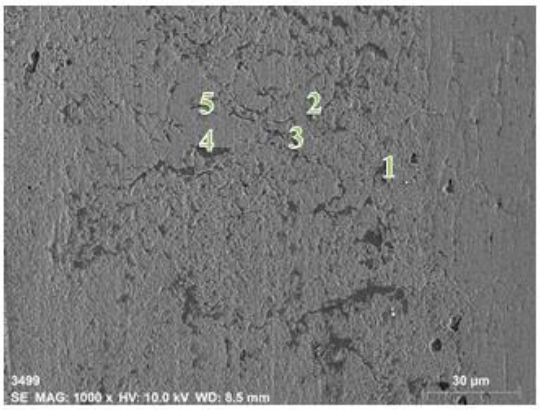

Mass percent (%)

Spectrum	C	O	V	Fe	Nb
1	7.25	49.58	0.20	42.31	0.66
2	32.99	39.44	0.00	27.40	0.18
3	25.09	53.21	0.00	21.69	0.00
4	5.23	30.36	0.00	63.58	0.83
5	4.85	5.00	0.08	87.77	2.30
Mean value:	15.08	35.52	0.06	48.55	0.80
Sigma:	13.08	19.26	0.09	27.26	0.91
Sigma mean:	5.85	8.61	0.04	12.19	0.41

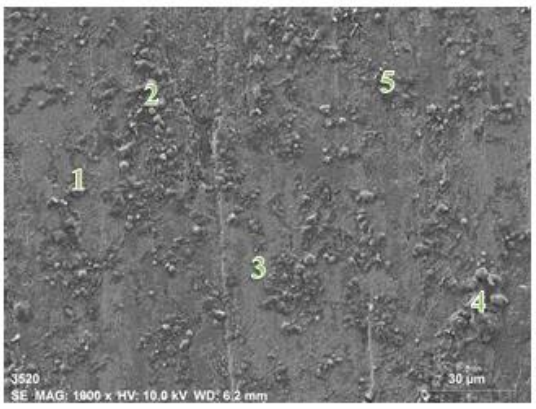

Mass percent (%)

Spectrum	C	O	V	Fe	Nb
1	3.08	42.70	0.00	54.08	0.14
2	6.22	44.43	0.00	49.35	0.00
3	4.28	24.80	0.28	70.64	0.00
4	6.49	45.81	0.12	47.30	0.27
5	6.37	43.56	0.00	49.55	0.51
Mean value:	5.29	40.26	0.08	54.19	0.18
Sigma:	1.53	8.72	0.12	9.53	0.21
Sigma mean:	0.69	3.90	0.06	4.26	0.10

Corrosive Nb-V

Figure 338. (continues).

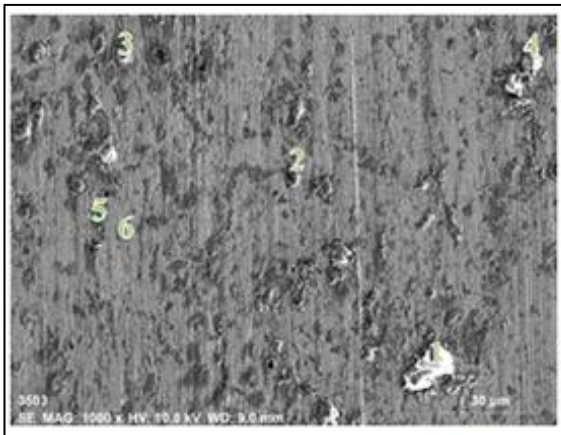

Mass percent (%)

Spectrum	C	O	Fe	Ni
1	9.52	55.69	30.01	4.78
2	4.73	57.30	33.90	4.07
3	3.99	56.71	35.43	3.87
4	13.47	53.00	29.98	3.54
5	7.69	52.88	31.72	7.71
6	9.41	10.60	70.55	9.44
Mean value:	8.14	47.70	38.60	5.57
Sigma:	3.49	18.27	15.80	2.42
Sigma mean:	1.43	7.46	6.45	0.99

Corrosive 5Ni

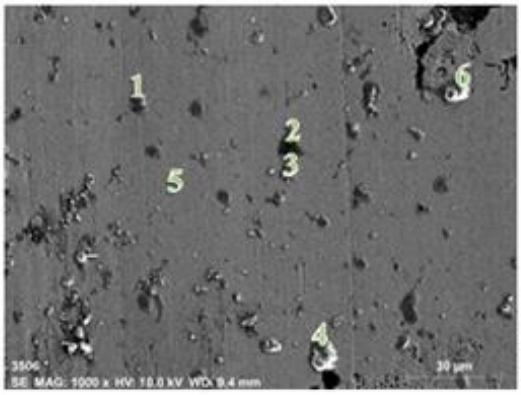

Mass percent (%)

Spectrum	C	O	V	Fe	Ni	Nb
1	1.78	46.62	0.00	49.13	2.36	0.11
2	34.81	23.14	0.07	37.80	4.18	0.00
3	7.01	50.92	0.20	36.38	5.50	0.00
4	0.83	41.09	0.25	57.24	0.59	0.00
5	4.26	3.81	0.00	77.94	14.00	0.00
6	7.00	51.26	0.00	37.91	3.67	0.16
Mean value:	9.28	36.14	0.09	49.40	5.05	0.05
Sigma:	12.76	18.95	0.11	16.20	4.69	0.07
Sigma mean:	5.21	7.74	0.05	6.61	1.92	0.03

Corrosive Nb-V 10Ni –15Newton

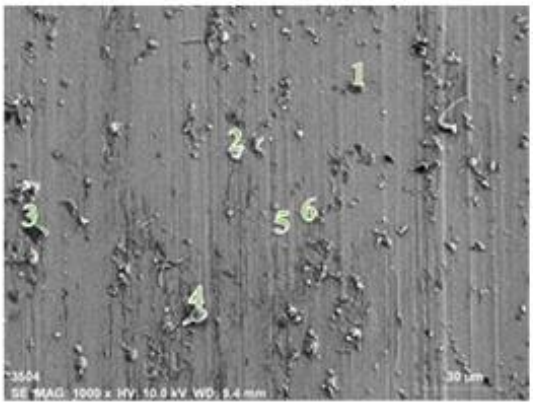

Mass percent (%)

Spectrum	C	O	V	Fe	Ni	Nb
1	2.93	45.48	0.36	46.10	5.13	0.00
2	4.98	42.86	0.30	46.63	5.23	0.00
3	9.08	42.77	0.61	44.61	2.80	0.12
4	7.90	22.81	0.59	62.78	5.51	0.41
5	6.51	7.41	1.32	72.33	12.26	0.18
6	9.60	10.18	0.30	72.95	6.70	0.25
Mean value:	6.83	28.59	0.58	57.57	6.27	0.16
Sigma:	2.55	17.38	0.39	13.42	3.20	0.16
Sigma mean:	1.04	7.10	0.16	5.48	1.31	0.06

Corrosive Nb-V 10Ni –30Newton

Figure 348. (continues).

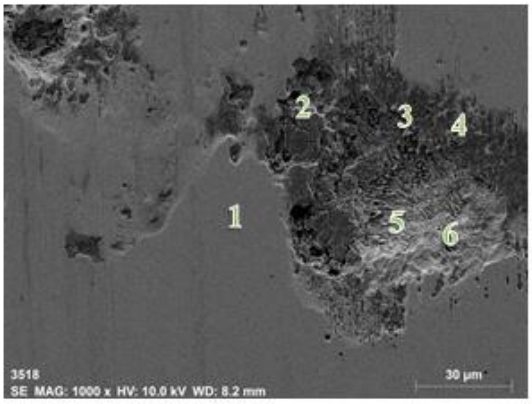

Mass percent (%)

Spectrum	C	O	V	Fe	Ni	Nb
1	4.01	1.64	0.60	80.10	13.65	0.00
2	5.85	47.54	0.25	41.36	5.00	0.00
3	7.97	5.66	0.35	84.45	1.56	0.00
4	4.80	48.51	0.36	38.30	8.03	0.00
5	6.69	4.06	0.06	80.70	8.49	0.00
6	17.58	13.21	0.00	61.33	7.87	0.00
Mean value:	7.81	20.11	0.27	64.37	7.44	0.00
Sigma:	4.98	21.97	0.22	20.67	4.02	0.00
Sigma mean:	2.03	8.97	0.09	8.44	1.64	0.00

Corrosive Nb-V 15Ni

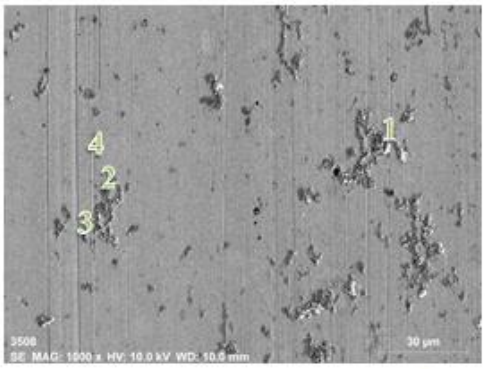

Mass percent (%)

Spectrum	C	O	V	Fe	Ni	Nb
1	5.32	55.64	0.19	24.80	13.99	0.05
2	5.56	51.68	0.17	26.88	15.39	0.30
3	7.49	49.80	0.00	25.96	16.67	0.08
4	6.30	4.75	0.00	62.60	26.07	0.29
Mean value:	6.17	40.47	0.09	35.06	18.03	0.18
Sigma:	0.97	23.94	0.10	18.38	5.47	0.13
Sigma mean:	0.49	11.97	0.05	9.19	2.73	0.07

Corrosive Nb-V-20Ni –15Newton

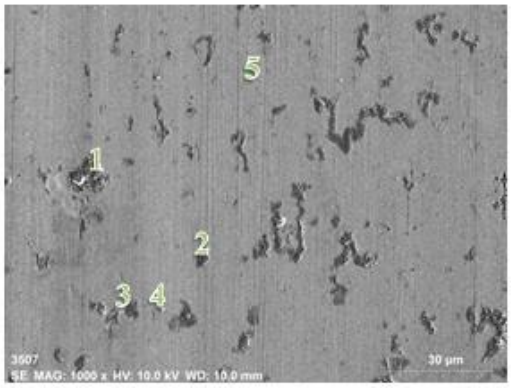

Mass percent (%)

Spectrum	C	O	V	Fe	Ni	Nb
1	1.50	51.68	0.84	40.43	5.55	0.00
2	3.62	50.94	0.33	31.35	13.76	0.00
3	5.30	39.41	0.00	41.04	14.25	0.00
4	17.53	41.45	0.00	36.98	4.04	0.00
5	4.23	3.19	0.50	58.74	33.22	0.11
Mean value:	6.43	37.33	0.34	41.71	14.17	0.02
Sigma:	6.35	19.86	0.36	10.27	11.62	0.05
Sigma mean:	2.84	8.88	0.16	4.59	5.20	0.02

Corrosive Nb-V-20ni –30Newton

Figure 358. (continues).

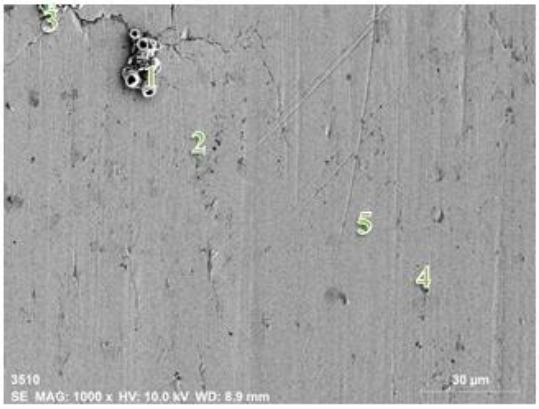

Mass percent (%)

Spectrum	C	O	V	Fe	Ni	Nb
1	5.15	52.11	0.00	23.23	19.51	0.00
2	6.53	32.62	0.31	23.52	37.02	0.00
3	6.41	43.49	0.41	28.70	20.76	0.23
4	2.59	51.18	0.48	23.44	22.31	0.00
5	3.94	1.79	0.23	56.71	37.12	0.21
Mean value:	4.92	36.24	0.28	31.12	27.34	0.09
Sigma:	1.68	20.78	0.19	14.49	8.93	0.12
Sigma mean:	0.75	9.29	0.08	6.48	4.00	0.05

Corrosive Nb-V-30ni –15 Newton

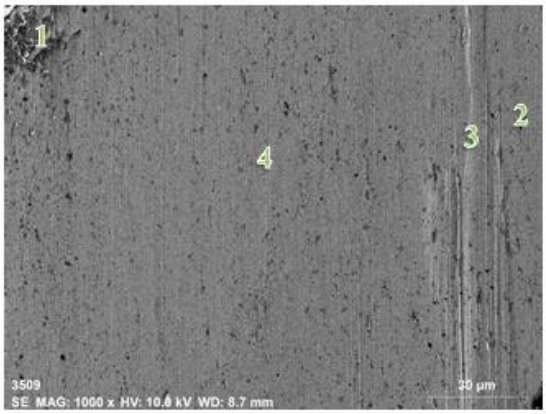

Mass percent (%)

Spectrum	C	O	V	Fe	Ni	Nb
1	7.03	47.71	0.00	21.31	23.95	0.00
2	6.92	5.14	0.66	55.49	31.78	0.00
3	4.56	6.86	0.00	42.62	45.97	0.00
4	4.23	2.07	0.13	48.92	44.47	0.17
Mean value:	5.69	15.44	0.20	42.08	36.54	0.04
Sigma:	1.50	21.60	0.32	14.81	10.54	0.09
Sigma mean:	0.75	10.80	0.16	7.41	5.27	0.04

Corrosive Nb-V-30Ni –30Newton

Figure 368. (continues).

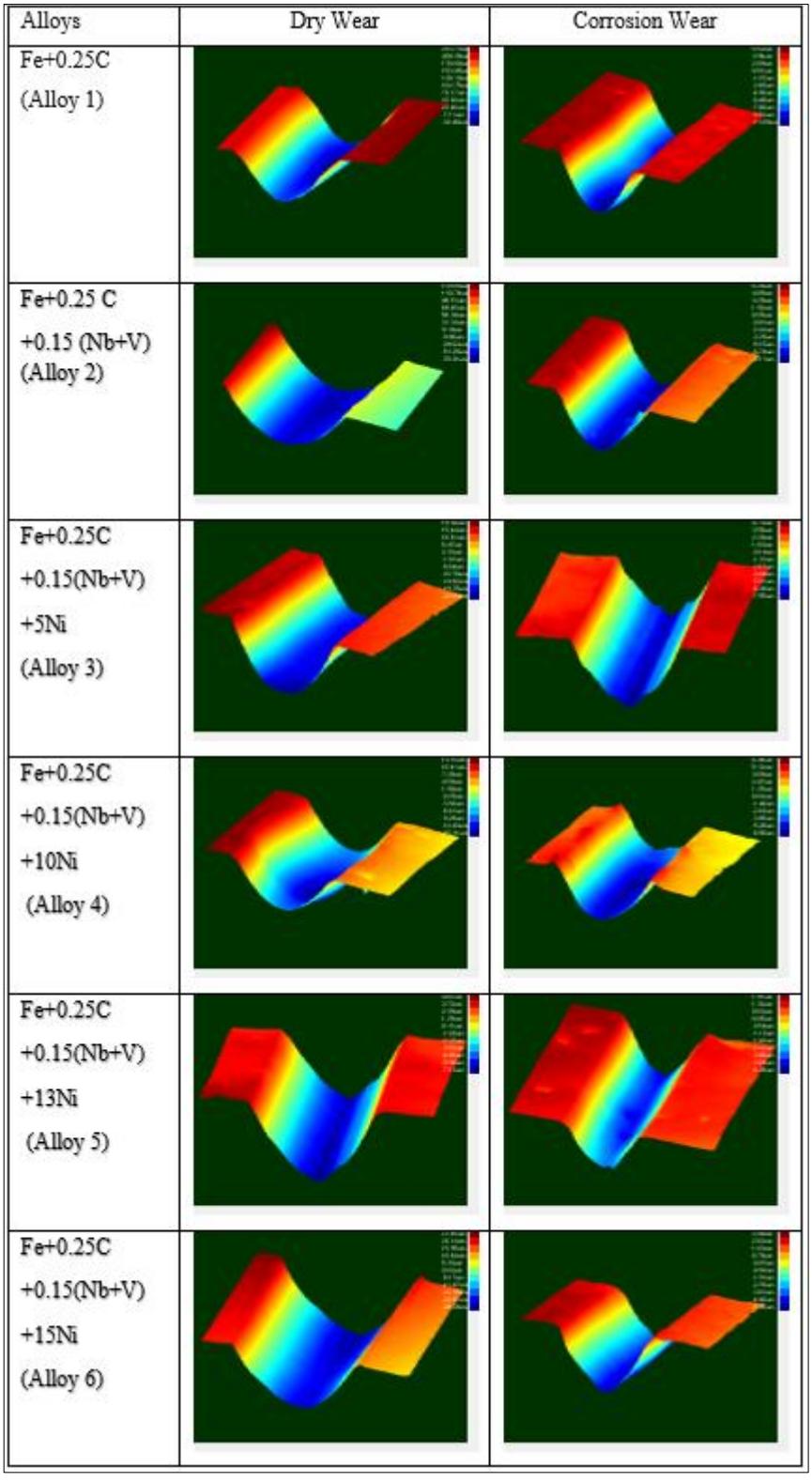

Figure 37. Topography images from worn surface of dry and corrosive conditions under 30N load.

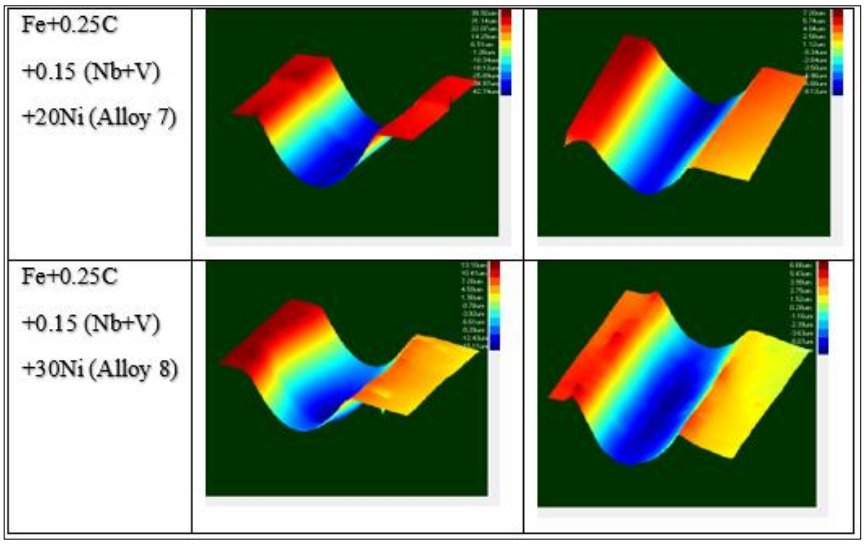

Figure 389. (continues).

Figure 29 displays the 3D topographic pictures that were obtained from the wear surfaces in order to more thoroughly investigate the wear outcomes. The topography images produced by coloring the 3D topographic photos in accordance with the variations in Ra values in wear zones made it easier to analyze the wear data.

Alloy 1 (Fe+0.25C) had a Ra value of 265 μm, in the wear test conducted under 30 N stress in a dry environment, however the same alloy's Ra value was measured as 16 μm in a corrosive environment [45].

The Alloy 5 (Fe+0.25C+0.15NbV+13Ni), which showed the least weight loss in wear testing, has Ra value 12 μm when tested under a 30 N load and 6.1m when tested in a corrosive environment, that because the corrosive fluid causes less deformation to the material's surface and internal structure, the high wear resistance in the corrosive environment manifests itself by lowering the weight loss during the wear test.

Ra value increased because the creation of uneven plastic deformation led to an increase in adhesion propensity in a dry wear environment. The abrasive wear behavior occurs in a more controlled manner because the corrosive wear fluid that enters the wear zone removes the heat from the wear environment. As a result, the material surface's quality improved.

This could occur as a result of the development of tiny precipitates, such as vanadium carbonitride (VCN) and niobium carbonitride (NbCN), either during the subsequent cooling phase or the 1400 °C sintering process. Nb and V precipitated out of the solution as grains and grain boundaries, according to the EDS research (Figure 30a, b). The EDS line analysis further demonstrates that the type and quantity of elements varied along the line crossing with the matrix and precipitates in Nb-V micro alloyed PM steels without Ni (alloy 2). It is well known that the precipitates discovered in alloys through SEM and EDS investigations significantly affect the growth and recrystallization of austenite grains [48,49].

The microalloying elements like V and Nb precipitate as niobium nitrite (NbN), niobium carbonitride (NbCN), and niobium carbide (NbC) while sintering or hot rolling followed by cooling that contributed to the hardness and tensile strength of the micro alloyed steels through solid solution hardening, precipitation hardening mechanisms, and grain refinement. The average grain sizes of alloys 1 and 2 that although alloy 1 had a grain size of 36.8 m, alloy 2's grain size reduced to 30.5m because of precipitates like NbC(N) and VC(N) during sintering. The precipitates did not let the austenite grains grow.

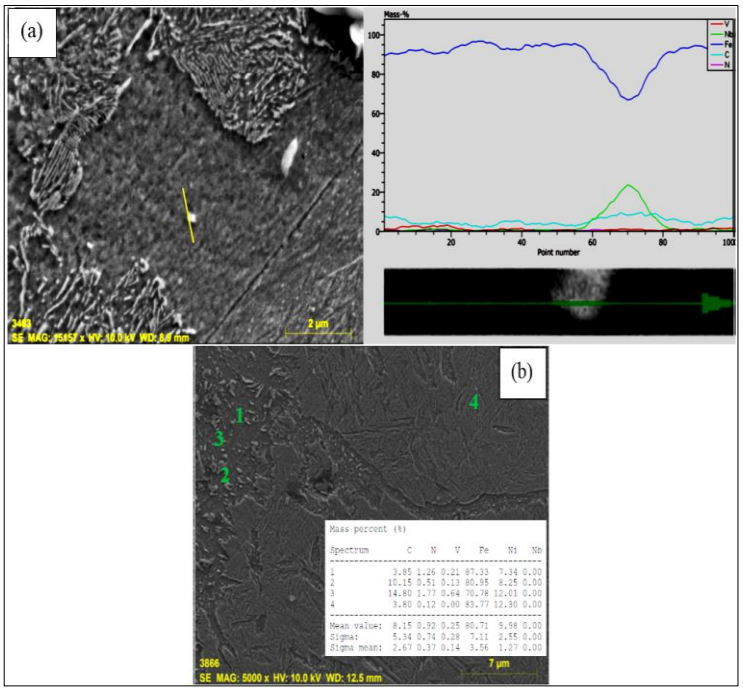

Figure 39. (a) SEM line EDS image of alloy 2 and (b) precpitates formed at grain boundaries.

The lamellar lengths of the cementite and austenite grains are shorter than those of the pearlite and pearlite, respectively, in bainitic structures, which are visible in the alloys' microstructures that contained 5% and 10% Ni. Furthermore, inhomogeneous microstructures appeared as a result of increased Ni concentrations. When the Ni concentration rose from 5% to 10%, localized Ni segregation occurred as a result of the decreased Ni diffusion coefficient; according to mapping analysis for alloys 3 and 4 in Figure 31. Elemental nickel diffuses into iron rather slowly because of its low diffusion coefficient, according to Tracey and Upadyaya's investigations [50]. As a result, there wasn't enough dispersion for the sintering process.

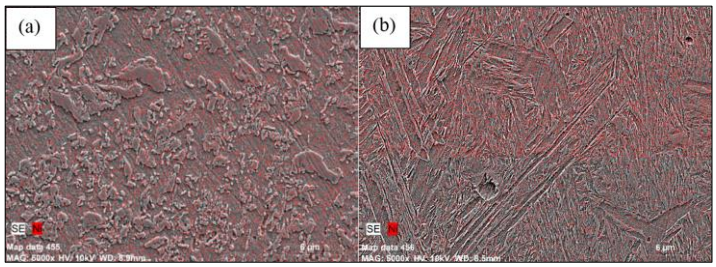

Figure 40. Elemental mapping for (a) alloy 3 and (b) alloy 4 sintered at 1400 °C.

In contrast to alloy 5-13Ni, alloy 6-15Ni features a needle-shaped martensitic structure next to the austenite grains. While the austenite grains make up the whole structure of the alloys 8-30Ni and 9-40Ni, the 7-20Ni alloy has a martensitic structure that is fairly close to the austenite grains.

The samples' post-sintering densities are about 93% because of their porosities. Pores may be present in powder-metallurgy-produced alloys [51]. Following sintering, the densities somewhat rose. The holes between the powder particles are reduced, the contact sites are enlarged, and the neck is formed during the sintering process. Grain boundaries form in the neck's regions. The uniformity of the material's structure increases with the width of the grain boundaries. In this study, it was discovered that as the amount of nickel grew, the microstructural porosity of the alloys increased. Alloy 8-30Ni exhibits more porosity than equivalent alloys with lower Ni

concentrations. The diverse alloy elements and variations in their sizes and shapes mean that low alloys are difficult to press and sinter.

It is believed that an increase in the amount of Ni added causes the bainitic and martensitic structure formation. Getting et al. investigated Ni addition and its effects on the mechanical properties of molybdenum PM steels. It was found that the Ni addition increased the PM steels' hardness and tensile strength, and harder phases are produced when nickel is added in 0-2% by weight. If nickel is given at a weight-based rate of 2% to 5%, the structure has a bainitic and martensitic structure [52].

6.3. GENERAL CONCLUSIONS

In this study, Fe-C-NbV-xNi alloys fabricated by powder metallurgy with and without Ni were characterized through microstructural observations, mechanical tests and corrosion tests. The following conclusions have been drawn. The results listed below were obtained from this study:

1. The alloy microstructures with Nb–V microalloyed steel without Ni and non-alloyed steel have pearlite and ferrite, but increasing Ni content formed intermetallic compounds (Fe3Ni2, FeNi3, and FeNi) and resulted in transformation to austenite.
2. The wear resistance increased with the addition of Ni up to the composition containing 13 Ni. A decrease in wear resistance was observed after the addition of 13 Ni, and this situation is compatible with the hardness values.
3. Although Ni has also been low in the alloys with 5, 10, 13, and 15Ni, the content almost systematically increased the corrosion resistance because of martensitic structure and possible microstructure inhomogeneity.

Moreover, in this investigation, microstructural analyses and wear testing were used to compare Fe-C-NbV-xNi alloys produced by powder metallurgy with and without Ni. The following findings were drawn:

1. Both of Ferrite and pearlite are found in the microstructures of alloys containing nonalloyed steel and Nb-V microalloyed steel without Ni. But as the Ni level rose, austenite changed and intermetallic complexes like Fe3Ni2 FeNi FeNi3 were formed.

2. The addition of Ni up to 13% enhanced the wear strength with hardness. It was increased further, which decreased the wear strength of the hardness
3. Since the corrosive fluid lessens the deformation on the material's surface and internal structure, the high wear resistance in the corrosive environment manifests itself by minimizing the weight loss during the wear test. Ra value increased because the creation of uneven plastic deformation led to an increase in adhesion propensity in a dry wear environment

6.3.1. Overall Results

The main aim that resulted from this study is to add Ni with a certain amount of alloyed and non-alloyed steel to produce a product with a higher wear resistance and a lower wear loss in the corrosive environment as well as enhanced alloy hardness.

REFERENCES

1. Ricciardi, A. P., Canfield, R. A., Patil, M. J., and Lindsley, N., "Nonlinear aeroelastic scaled-model design", ***Journal Of Aircraft***, 53(1): 20–32 (2016).

2. Ebrahimi, A. and Moshksar, M. M., "Evaluation of machinability in turning of microalloyed and quenched-tempered steels: Tool wear, statistical analysis, chip morphology", ***Journal of materials processing technology***, 209(2): 910-921 (2009).

3. Wang, X. Y., Wen, Z. X., Cheng, H., Gu, S. N. and Lu, G. X., "Influences of the heating and cooling", ***Metals***, 9(3): (2019).

4. Anand, S., Schade, R. R., Bendetti, C., Kelly, R., Rabin, B. S., Krause, J., Starzl, T. E., Iwatsuki, S. and Van Thiel, D. H., "Idiopathic Hemochromotosis and Alpha-1-Antitrypsin Deficiency: Coexistence in a Family with Progressive Liver Disease in the Proband", ***Hepatology***, 3(5): 714–718 (1983).

5. Erden, M. A., Erer, A. M., Odabaşi, Ç. and Gündüz, S., "The investigation of the effect of cu addition on the Nb-V microalloyed steel produced by powder metallurgy", ***Science of Sintering***, 54(2): 153-167 (2022).

6. Gündüz, S., Erden, M.A., Karabulut, H. and Türkmen, M., "Effect of the addition of niobium and aluminium on the microstructures and mechanical properties of micro-alloyed PM steels", ***Mater. Teh.***, 50, 641–648 (2016).

7. H. A. Raghs, B. Kondul, M. H. Cetin "Investigation of Wear Behavior of Boronized H13 Steel under Environment of Nano-Silver-Added Lubricants Coated with Different Ligands", ***Surface Topography: Metrology and Properties***, 1-34 (2020).

8. Demirtaş, H. and Erden, M., "Cr ve Ni İlavesinin Sade Karbonlu Çeliğin Mekanik Özelliklerine Etkisi", ***Düzce Üniversitesi Bilim ve Teknoloji Dergisi***, 7 (3): 1217-1223 (2019).

9. Coovattanachai, O., Lasutta, P., Tosangthum, N. and Krataitong, R., "Analysis of Compaction and Sintering of Stainless Steel Powders", ***Chiang Mai J. Sci***, 33(2): 293-300 (2006).

10. Cai, J., Lin, J. and Wilsius, J., "Modelling phase transformations in hot stamping and cold die quenching of steels. In Microstructure Evolution in Metal Forming Processes", ***Woodhead Publishing***, Sawston, 210-236 (2012).

11. Baker, T. N., "Microalloyed steels", ***Ironmaking & Steelmaking***, 43(4): 264-307 (2016).

12. Web: Wikipedia, "Microalloyed steel", **https://en.wikipedia.org/wiki/Microalloyed_steel** (2022).

13. Web: Wikipedia, "Vanadyum pentoksit", **https://tr.wikipedia.org/wiki/Vanadyum_pentoksit** (2022).

14. Web: Wikipedia, "Alüminyum", **https://tr.wikipedia.org/wiki/Al%C3%BCminyum** (2022).

15. Web: Wikipedia, "Niyobyum", **https://tr.wikipedia.org/wiki/Niyobyum** (2022).

16. Web: Wikipedia, "Karbon", **https://tr.wikipedia.org/wiki/Karbon** (2022).

17. Web: Wikipedia, "Nitrogen", **https://en.wikipedia.org/wiki/Nitrogen** (2022).

18. Web: Wikipedia, "Silisyum", **https://tr.wikipedia.org/wiki/Silisyum** (2022).

19. Web: Wikipedia, "Fosfor", **https://tr.wikipedia.org/wiki/Fosfor** (2022).

20. Web: Wikipedia, “Manganez”, **https://tr.wikipedia.org/wiki/Manganez** (2022).

21. Web: Wikipedia, “Nikel”, **https://tr.wikipedia.org/wiki/Nikel** (2022).

22. Fischmeister, H. F., "Applications of quantitative microscopy in materials engineering", J***ournal of Microscopy***, 95(1): 119-143 (1972).

23. Aparova, A. I., Lyapunov, A. I. and Eremin, V. I., "Effect of nickel and manganese on the structure and properties of steel R3M3F2", ***Metal Science and Heat Treatment***, 29: 124-128 (1987).

24. Web: Wikipedia, “Grain boundary strengthening”, **https://en.wikipedia.org/wiki/Grain_boundary_strengthening#:~:text=Decreasing%20grain%20size%20decreases%20the,the%20higher%20the%20yield%20strength** (2022).

25. Web: Wikipedia, “Precipitation hardening”, **https://en.wikipedia.org/wiki/Precipitation_hardening** (2022).

26. Majta, J., Lenard, J. G. and Pietrzyk, M., "A study of the effect of the thermomechanical history on the mechanical properties of a high niobium steel", ***Materials Science and Engineering: A***, 208(2): 249-259 (1996).

27. Web: Wikipedia, “Powder metallurgy”, **https://en.wikipedia.org/wiki/Powder_metallurgy** (2022).

28. Cooke, A. and Slotwinski, J., "Properties of metal powders for additive manufacturing: A review of the state of the art of metal powder property testing", ***Additive Manufacturing Materials: Standards, Testing And Applicability***, 21-48 (2015).

29. Hangai, Y., Zushida, K., Fujii, H., Ueji, R., Kuwazuru, O. and Yoshikawa, N., "Friction powder compaction process for fabricating open-celled Cu foam by sintering-dissolution process route using NaCl space holder", ***Materials Science and Engineering: A***, 585: 468-474 (2013).

30. Akdoğan, E., "Investigation of the Effects of Unidirectional Compression on the Hardness of High-Density Polyethylene Materials", ***Open Journal of Nano***, 7(2): 94-103 (2022).

31. James, P. J., "Particle deformation during cold isostatic pressing of metal powders", ***Powder Metallurgy***, 20(4): 199-204 (1977).

32. Ramesh Babu, S., Jaskari, M., Järvenpää, A. and Porter, D., "The effect of hot-mounting on the microstructure of an As-Quenched auto-tempered low-carbon martensitic steel", ***Metals***, 9(5): 550 (2019).

33. ASTM, G., "Standard practice for calculation of corrosion rates and related information from electrochemical measurements", ***ASTM International***: West Conshohocken, PA, USA (2010).

34. Bai, Q., Zou, Y., Kong, X., Gao, Y., Dong, S. and Zhang, W., "The influence of the corrosion product layer generated on the high strength low-alloy steels welded by underwater wet welding with stainless steel electrodes in seawater", ***Journal of Ocean University of China***, 16: 49-56 (2017).

35. Türkmen, M., Karabulut, H., Erden, M. A. and Gündüz, S., "Effect of TiN addition on The microstructure and mechanical properties of PM steels", ***Technological Applied Sciences***, 12(4): 178-184 (2017).

36. Schwerdtfeger, W. J., "Corrosion rates of binary alloys of nickel and iron measured by polarization methods", ***NBS J RES ENG INSTRUM***, 70(3): 187-194 (1966).

37. Marsh, J.S. "Alloys of Iron and Nickel", ***McGraw-Hill Publishing Company***, New York (1938).

38. Alharthi, N., Sherif, E.-S.M., Abdo, H.S. and El Abedin, S.Z., "Effect of Nickel Content on the Corrosion Resistance of Iron-Nickel Alloys in Concentrated Hydrochloric Acid Pickling Solutions", ***Adv. Mater. Sci. Eng***., 1-8 (2017).

39. Ahssi, M. A. M., Erden, M. A., Acarer, M. and Çuğ, H., "The effect of nickel on the microstructure, mechanical properties and corrosion properties of niobium–vanadium microalloyed powder metallurgy steels", ***Materials***, 13(18): 4021 (2020).

40. Türkmen, M., Erden, M., Karabulut, H. and Gündüz, S., "The Effects of Heat Treatment on the Microstructure and Mechanical Properties of Nb-V Microalloyed Powder Metallurgy Steels", ***Acta Phys. Pol.***, 135: 834–836 (2019).

41. Erden, M. A., Gündüz, S., Karabulut, H. and Türkmen, M., "Wear behaviour of sintered steels obtained using powder metallurgy method", ***Mechanics***, 23(4): 574-580 (2017).

42. Erden, M. A., "The effect of sintering time on tensile strength of NB-V microalloyed powder metallurgy steels", ***Technological Applied Sciences***, 15(1): 15-22 (2020).

43. Noskov, A.I., Gilmutdinov, A.K. and Yanbaev, R.M., "Effect of coaxial laser cladding parameters on bead formation", ***Int. J. Miner. Met. Mater***. 24: 550-556 (2017).

44. Upadhyaya, G. S., "Sintered Metallic and Ceramic Materials-Sintered Low-Alloy Ferrous Materials", ***John Wiley & Sons LTD***, West Sussex, UK (2000).

45. Alharthi, N., Sherif, E.-S.M., Abdo, H.S. and El Abedin, S.Z., "Effect of Nickel Content on the Corrosion Resistance of Iron-Nickel Alloys in Concentrated Hydrochloric Acid Pickling Solutions", ***Adv. Mater. Sci. Eng***. (2017).

46. Tracey, V., "Nickel sintered steels-Developments, status and prospects", ***Met. Powder Rep***. (1992).

RESUME

Mohamed ahmed AHSSI had completed his elementary, middle and high school in zentane city –Libya country. After that he joined the undergraduate programmed in the University of Tripoli as a student in Mechanical Engineering and Industrial department in 1996, and graduated in 2001 with Bachelor Degree. In the 2013, he began his postgraduate studies at Sheffield Hallam University UK as a master's student in the department of Mechanical Engineering and Industrial and graduated in 2015. In the 2018 he started his postgraduate studies at Karabuk University as doctorate student in the department of Mechanical Engineering.